Progress of Theoretical Physics, Vol. 20, No. 1, July 1958

Theory of Line-Shapes of the Exciton Absorption Bands

Yutaka TOYOZAWA

Research Institute for Fundamental Physics, Kyoto University, Kyoto

(Received April 12, 1958)

A general theory of line-shapes of the exciton absorption bands is developed with the help of generating function method. When the exciton-lattice coupling is weak, and the exciton effective mass is small, the absorption band is of a Lorentzian shape, provided that the temperature T is not too high. The half-value width H is given by the level broadening of the optically produced $\boldsymbol{K}=0$ exciton due to lattice scattering, so that it is proportional to T except at low temperatures. If the coupling is strong, or the exciton effective mass is large, or the temperature is very high, the absorption band is expected to be of a Gaussian shape, and H is proportional to $\sqrt{T}$. The mutual influence of adjacent absorption bands is also discussed; it causes the asymmetry and repulsion of the components as temperature rises.

If we replace T by the density of lattice imperfections, the above statements are valid, without substantial modifications, as regards the dependence on the degree of imperfections.

These conclusions are in qualitative agreement with experimental data. The comparison further provides us with information on the strength of the exciton-lattice coupling and the energy band structure of the exciton.

§ 1. Introduction

Since the "exciton" model was first introduced by Frenkel,[1] and was applied to the explanation of several sharp peaks which are observed on the low energy sides of characteristic absorption bands in typical insulating crystals, most of theoretical attention was directed to the electronic structure of the exciton.[2)-8)] Results of calculations can be compared with the experimental data, as regards peak positions,[2)-5)] oscillator strengths,[6)] multiplet structures[7),8)] and so on. However, the observed peak position corresponds to the energy of the exciton with wave number $\boldsymbol{K}$ nearly equal to zero, so that it does not directly give us the information on the energy band structure of the exciton.

On the other hand, the problem of exciton-phonon interaction has been attacked by several authors; some dealt with the stationary state problem of the exciton phonon system,[9),10)] while others calculated the probability for the scattering of an exciton by phonons.[11)] To relate these results directly with experimental data seems rather difficult, at least in the present stage.

As for the line-shapes of the exciton absorption bands, however, it does not seem that remarkable progress bas been made on the theoretical side since the pioneer work by Peierls.[12)] It is the purpose of the present paper to develop a general theory of the line-shape in such a way that as much information as possible is obtained through comparison with experiments. We also wish that it could contribute to inter-relating more closely the theoretical and experimental works stated above.

In § 2 of this paper, the exciton-lattice interaction Hamiltonian H_{eL} is derived with Wannier's exciton wave function, including the effective mass approximation as a special case. A general formula for the optical absorption coefficient of this electron (exciton)-lattice system is derived, in § 3, as a function of the radiation frequency. The Fourier transform of the absorption coefficient, that is, the generating function, is expanded into an infinite power series H_{eL}. In the two extreme cases, that is, weak and strong limits of the coupling H_{eL}, the series can be brought into simpler expressions. Thus, in the limit of weak coupling (§ 4), the absorption band tends to a Lorentzian shape due to the motional effect of the exciton. In the opposite limit the band takes a Gaussian shape, which means that the "localized exciton" model is valid in this case (§ 5). In the intermediate region, the absorption band may show an asymmetry, depending upon the energy band structure of the exciton.

When two or more exciton absorption bands lie very close to each other, the influence of each component on the strengths, peak positions and shape asymmetries of other components becomes important, as is discussed in § 6.

§ 7 is devoted to the derivation of criterion for the appearance of two extreme cases in a more explicit form, and to the arrangement of theoretical conclusions so as to be convenient for comparison with experimental data. In § 8 we carried out the analysis of a few of experimental data available, which proves to be in satisfactory agreement with theoretical expectations.

Further information is obtained through this comparison: one is the strength of the exciton-lattice coupling, and the other concerns the energy band structure of the exciton. They will be utilized, in the next paper, for speculative investigations of the various dynamical processes which the exciton possibly suffers.[13]

§ 2. The derivation of exciton-lattice interaction Hamiltonian

Let us consider an insulating crystal consisting of N atoms and N valence electrons, and denote the Wannier functions[4] for valence and conduction bands by $a_v(\boldsymbol{x}, m)$ and $a_c(\boldsymbol{x}, n)$, respectively, where m and n refer to lattice sites.

In the approximation of one electron excitation, the wave function for an exciton with inner quantum number λ and translational wave-number $\boldsymbol{K}$ is given by[4]

$$\Psi_{\lambda K}=N^{-1/2}\sum_{m}\exp(i\boldsymbol{K}\cdot\boldsymbol{m})\sum_{l}U_{\lambda K}(\boldsymbol{l})\,A(\boldsymbol{m}, \boldsymbol{m}+\boldsymbol{l}), \qquad (2\cdot1)$$

where $A(\boldsymbol{m}, \boldsymbol{n})$ is the Slater determinant of N electrons for the configuration $[a_v(\boldsymbol{x}, 1), a_v(\boldsymbol{x}, 2), \cdots a_v(\boldsymbol{x}, m-1), a_c(\boldsymbol{x}, n), a_v(\boldsymbol{x}, m+1)\cdots, a_v(\boldsymbol{x}, N)]$, that is, the configuration in which the valence electron of the m-th site is excited into the conduction band, at the n-th site. The wave function $U_{\lambda K}(\boldsymbol{l})$ for the relative motion of the electron and the hole is to be determined from Wannier's difference equation, with Hamiltonian $H_{ex}=T+V$, where T is the sum of the energies of the electron and the hole, and V denotes Coulomb and exchange interactions between them.

If we make use of the effective mass approximation, the kinetic term T, as an operator on $U_{\lambda K}(\boldsymbol{l})$, can be replaced by a differential operator $W(-i\cdot\partial/\partial\boldsymbol{l}, \boldsymbol{K})$, where

$$W(\boldsymbol{k},\ \boldsymbol{K}) \equiv -W_v(\boldsymbol{k}-\boldsymbol{K}) + W_c(\boldsymbol{k}), \tag{2·2}$$

and $W_v(\boldsymbol{k})$, $W_c(\boldsymbol{k})$ mean the one electron energies, with wave number $\boldsymbol{k}$, of the valence and conduction bands, respectively. For a fixed value of $\boldsymbol{K}$, one can expand $W(\boldsymbol{k},\ \boldsymbol{K})$ around a minimum point $\boldsymbol{k}_m(\boldsymbol{K})$:

$$W(\boldsymbol{k},\ \boldsymbol{K}) = J(\boldsymbol{K}) + (\boldsymbol{k}-\boldsymbol{k}_m(\boldsymbol{K}))\cdot\hbar^2/2\mu(\boldsymbol{K})\cdot(\boldsymbol{k}-\boldsymbol{k}_m(\boldsymbol{K})) + \cdots, \tag{2·3}$$

the coefficient $\mu(\boldsymbol{K})$ being a reduced mass tensor. If we transform the wave function by

$$\varphi_{\lambda\boldsymbol{K}}(\boldsymbol{l}) = e^{-i\boldsymbol{k}_m(\boldsymbol{K})\boldsymbol{l}}U_{\lambda\boldsymbol{K}}(\boldsymbol{l}), \tag{2·4}$$

T is replaced by

$$J(\boldsymbol{K}) - \partial/\partial\boldsymbol{l}\cdot\hbar^2/2\mu(\boldsymbol{K})\cdot\partial/\partial\boldsymbol{l}. \tag{2·5}$$

The potential part V, in this new representation, is written as

$$\begin{aligned}
&(\boldsymbol{l}\,|\,V\,|\,\boldsymbol{l}')\\
&= -e^{i\boldsymbol{k}_m(\boldsymbol{K})(\boldsymbol{l}-\boldsymbol{l}')}\sum_{\boldsymbol{\rho}} e^{i\boldsymbol{K}\boldsymbol{\rho}}\iint a_v(\boldsymbol{x},\ 0)\,a_v^*(\boldsymbol{x},\ \boldsymbol{\rho})\\
&\times e^2/|\boldsymbol{x}-\boldsymbol{x}'|\cdot a_c^*(\boldsymbol{x}',\ \boldsymbol{l})\,a_c(\boldsymbol{x}',\ \boldsymbol{\rho}+\boldsymbol{l}')\,d\boldsymbol{x}\,d\boldsymbol{x}'\\
&+ e^{i\boldsymbol{k}_m(\boldsymbol{K})(\boldsymbol{l}-\boldsymbol{l}')}\sum_{\boldsymbol{\rho}} e^{i\boldsymbol{K}\boldsymbol{\rho}}\iint a_v(\boldsymbol{x},\ 0)\,a_v^*(\boldsymbol{x}',\ \boldsymbol{\rho})\\
&\times e^2/|\boldsymbol{x}-\boldsymbol{x}'|\cdot a_c^*(\boldsymbol{x},\ \boldsymbol{l})\,a_c(\boldsymbol{x}',\ \boldsymbol{\rho}+\boldsymbol{l}')\,d\boldsymbol{x}\,d\boldsymbol{x}'.
\end{aligned} \tag{2·6}$$

It reduces to a Coulomb attraction $-\delta_{ll'}e^2/|l|$ in the crudest approximation, as is well known.

If we make further simplification by taking parabolic approximation for both of the energy bands:

$$\begin{aligned}
W_v(\boldsymbol{k}) &= -(\boldsymbol{k}-\boldsymbol{k}_v)\cdot\hbar^2/2m_h\cdot(\boldsymbol{k}-\boldsymbol{k}_v),\\
W_c(\boldsymbol{k}) &= \varepsilon_g + (\boldsymbol{k}-\boldsymbol{k}_c)\cdot\hbar^2/2m_e\cdot(\boldsymbol{k}-\boldsymbol{k}_c),
\end{aligned} \tag{2·7}$$

we have

$$\begin{aligned}
\boldsymbol{k}_m(\boldsymbol{K}) &= p_h\cdot(\boldsymbol{k}_v+\boldsymbol{K}) + p_e\cdot\boldsymbol{k}_c,\\
J(\boldsymbol{K}) &= \varepsilon_g + \boldsymbol{K}^*\cdot\hbar^2/2m^*\cdot\boldsymbol{K}^*,
\end{aligned} \tag{2·8}$$

where

$$\begin{aligned}
&m^* \equiv m_e+m_h, \quad \mu^{-1} \equiv m_h^{-1}+m_e^{-1},\\
&p_h \equiv \mu\cdot m_h^{-1} = m_e\cdot m^{*-1}, \quad p_e \equiv \mu\cdot m_e^{-1} = m_h\cdot m^{*-1},\\
&\boldsymbol{K}^* \equiv \boldsymbol{K}-\boldsymbol{K}_0, \quad \boldsymbol{K}_0 \equiv \boldsymbol{k}_c-\boldsymbol{k}_v.
\end{aligned} \tag{2·9}$$

The result is shown in Fig. 1 schematically. Because of symmetry, of course, there are actually equivalent branches on the opposite sides.

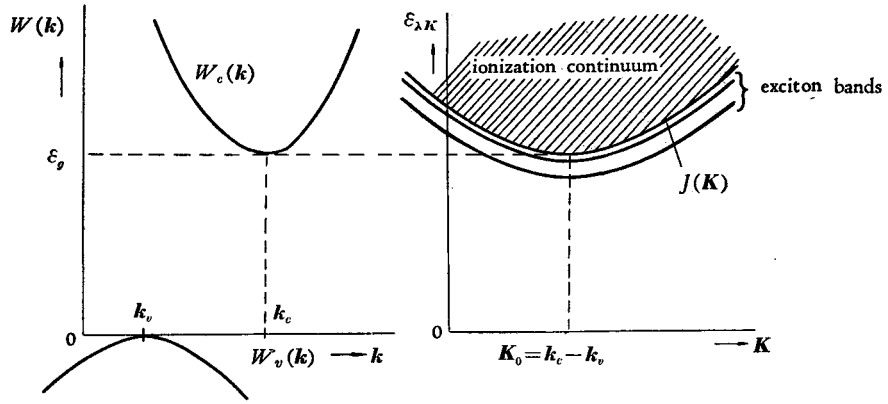

(a) One electron energy levels. (b) Energy states for one electron excitation of N-electron system.

Fig. 1. Energy level scheme in the effective mass approximation.

We now consider the change of the potential energy between electrons and lattice, caused by an arbitrary lattice deformation: it is the sum of N equivalent one-electron energies:

$$\delta H_e(\boldsymbol{x}_1, \boldsymbol{x}_2, \cdots, \boldsymbol{x}_N) = \sum_{i=1}^{N} \delta H_1(\boldsymbol{x}_i). \tag{2·10}$$

Making use of the relation

$$(A(\boldsymbol{m}, \boldsymbol{n}) |\delta H_e| A(\boldsymbol{m}', \boldsymbol{n}')) = -\delta_{nn'} \int a_v(\boldsymbol{x}, \boldsymbol{m}) \delta H_1 \times a_v^*(\boldsymbol{x}, \boldsymbol{m}') d\boldsymbol{x} + \delta_{mm'} \int a_c^*(\boldsymbol{x}, \boldsymbol{n}) \delta H_1 a_c(\boldsymbol{x}, \boldsymbol{n}') d\boldsymbol{x},$$

and then transforming the Wannier functions into the Bloch orbitals $b_v(\boldsymbol{x}, \boldsymbol{k})$ and $b_c(\boldsymbol{x}, \boldsymbol{k})$, we have

$$\begin{aligned}(\Psi_{\lambda \boldsymbol{K}} |\delta H_e| \Psi_{\lambda' \boldsymbol{K}'}) &= -N^{-1} \sum_{\boldsymbol{l}} \sum_{\boldsymbol{l}'} \sum_{\boldsymbol{k}} U_{\lambda \boldsymbol{K}}^*(\boldsymbol{l}) U_{\lambda' \boldsymbol{K}'}(\boldsymbol{l}') \exp\{i(\boldsymbol{K}+\boldsymbol{k})(\boldsymbol{l}-\boldsymbol{l}')\} \\ &\times \Xi_v(\boldsymbol{k}+\boldsymbol{K}-\boldsymbol{K}', \boldsymbol{k}) + N^{-1} \sum_{\boldsymbol{l}} \sum_{\boldsymbol{l}'} \sum_{\boldsymbol{k}} U_{\lambda \boldsymbol{K}}^*(\boldsymbol{l}) U_{\lambda' \boldsymbol{K}'}(\boldsymbol{l}') \\ &\times \exp\{i(\boldsymbol{K}-\boldsymbol{K}')\boldsymbol{l}' + i\boldsymbol{k}(\boldsymbol{l}-\boldsymbol{l}')\} \Xi_c(\boldsymbol{k}, \boldsymbol{k}-\boldsymbol{K}+\boldsymbol{K}'),\end{aligned} \tag{2·11}$$

where

$$\Xi_v(\boldsymbol{k}, \boldsymbol{k}') \equiv \int b_v^*(\boldsymbol{x}, \boldsymbol{k}) \delta H_1(\boldsymbol{x}) b_v(\boldsymbol{x}, \boldsymbol{k}') d\boldsymbol{x} \tag{2·12}$$

is the usual scattering matrix element of an electron-lattice system.

The lattice distortion, which causes $\delta H_1(\boldsymbol{x})$, may be an instantaneous position of thermal vibration, or a static deformation due to any kind of lattice imperfections such

as dislocations. For the acoustic mode of vibration we can take (i) the *deformable atom approximation* due to Bloch and Bethe[14] or (ii) the *deformation potential* introduced by Bardeen and Shockley,[15] as the case may be. In the case of optical mode of vibration in ionic crystals, δH_1 is nothing but the electrostatic field due to the polarization of the lattice, and was given by (iii) Fröhlich *et al.*[16] Throughout these three cases (2·12) depends only on $(\boldsymbol{k}-\boldsymbol{k}')$, that is, $\Xi_v(\boldsymbol{k},\boldsymbol{k}')\equiv\xi_v(\boldsymbol{k}-\boldsymbol{k}')$, and (2·11) is written as

$$-q_h(\lambda\boldsymbol{K},\ \lambda'\boldsymbol{K}')\xi_v(\boldsymbol{K}-\boldsymbol{K}')+q_e(\lambda\boldsymbol{K},\ \lambda'\boldsymbol{K}')\xi_c(\boldsymbol{K}-\boldsymbol{K}'). \tag{2·13}$$

If one takes the effective mass approximation (2·2)$\sim$(2·9), which is tacitly assumed also when one calculates (2·12) in the three cases (i)$\sim$(iii) stated above, q can be expressed as

$$\left.\begin{aligned} q_h(\lambda\boldsymbol{K},\ \lambda'\boldsymbol{K}') &\equiv \sum_l U_{\lambda\boldsymbol{K}}^*(\boldsymbol{l})\,U_{\lambda'\boldsymbol{K}'}(\boldsymbol{l}) \\ &= \sum_l \varphi_\lambda^*(\boldsymbol{l})\,\varphi_{\lambda'}(\boldsymbol{l})\exp\{-i(\boldsymbol{K}-\boldsymbol{K}')\cdot p_h\cdot\boldsymbol{l}\}\equiv q_h(\boldsymbol{K}-\boldsymbol{K}';\ \lambda\lambda'), \\ q_e(\lambda\boldsymbol{K},\ \lambda'\boldsymbol{K}') &\equiv \sum_l U_{\lambda\boldsymbol{K}}^*(\boldsymbol{l})\,U_{\lambda'\boldsymbol{K}'}(\boldsymbol{l})\exp\{i(\boldsymbol{K}-\boldsymbol{K}')\cdot\boldsymbol{l}\} \\ &= \sum \varphi_\lambda^*(\boldsymbol{l})\,\varphi_{\lambda'}(\boldsymbol{l})\exp\{+i(\boldsymbol{K}-\boldsymbol{K}')\cdot p_e\cdot\boldsymbol{l}\}\equiv q_e(\boldsymbol{K}-\boldsymbol{K}';\ \lambda\lambda'). \end{aligned}\right\} \tag{2·14}$$

We now introduce, for convenience, the creation-annihilation operators $a_{\lambda\boldsymbol{K}}^*$, $a_{\lambda\boldsymbol{K}}$ for the $(\lambda\boldsymbol{K})$-exciton, whose energy we denote by $\varepsilon_{\lambda\boldsymbol{K}}$, and the creation-annihilation operators $b_{\mu\boldsymbol{w}}^*$, $b_{\mu\boldsymbol{w}}$ for the $(\mu\boldsymbol{w})$-phonon with energy quantum $\hbar\omega_{\mu\boldsymbol{w}}$, where μ and $\boldsymbol{w}$ refer to the mode and the wave number of the phonon. a and a^* satisfy approximately the commutation relations for bosons, but this is immaterial as far as we confine ourselves to the electronic states in which the total number of excitons is zero or unity, as we do in later discussions. The Hamiltonian of the electron system and that of the lattice system are now written as

$$\left.\begin{aligned} H_e &= \sum_{\lambda\boldsymbol{K}}\varepsilon_{\lambda\boldsymbol{K}}\,a_{\lambda\boldsymbol{K}}^*\,a_{\lambda\boldsymbol{K}}, \\ H_L &= \sum_{\mu\boldsymbol{w}}\hbar\omega_{\mu\boldsymbol{w}}\,b_{\mu\boldsymbol{w}}^*\,b_{\mu\boldsymbol{w}}, \end{aligned}\right\} \tag{2·15}$$

respectively, whereas the interaction between them is written, in linear approximation but otherwise quite generally, as

$$H_{eL}=\sum_\mu\sum_{\lambda\boldsymbol{K}}\sum_{\lambda'\boldsymbol{K}'} i(\lambda\boldsymbol{K}|\beta_\mu|\lambda'\boldsymbol{K}')\,(b_{\mu,\boldsymbol{K}-\boldsymbol{K}'}-b_{\mu,-\boldsymbol{K}+\boldsymbol{K}'}^*)\,a_{\lambda\boldsymbol{K}}^*\,a_{\lambda'\boldsymbol{K}'}. \tag{2·16}$$

In the three cases (i)$\sim$(iii) stated above, we have explicit expressions for the matrix element (2·12), and $(\lambda\boldsymbol{K}|\beta_\mu|\lambda'\boldsymbol{K}')$ depends on $\boldsymbol{K}$ and $\boldsymbol{K}'$ only through $\boldsymbol{K}-\boldsymbol{K}'$ as is seen from (2·13) and (2·14). If we write $(\lambda\boldsymbol{K}|\beta_\mu|\lambda'\boldsymbol{K}')=\beta_\mu(\boldsymbol{K}-\boldsymbol{K}';\ \lambda\lambda')$, it is given by

$$\left.\begin{aligned} \beta_{ac}(\boldsymbol{w};\ \lambda\lambda') &= (2\hbar/9NMu)^{1/2}w^{1/2}\{-q_h(\boldsymbol{w};\ \lambda\lambda')\,C_v+q_e(\boldsymbol{w};\ \lambda\lambda')\,C_c\}, \\ \beta_{op}(\boldsymbol{w};\ \lambda\lambda') &= \{2\pi\hbar\omega e^2/Nv_0\cdot(1/\kappa_0-1/\kappa)\}^{1/2}1/w\cdot\{-q_h(\boldsymbol{w};\ \lambda\lambda')+q_e(\boldsymbol{w};\ \lambda\lambda')\}, \end{aligned}\right\} \tag{2·17}$$

for the acoustic and optical modes, respectively. In case (i) C is nothing but the kinetic energy of the Bloch function, whereas in case (ii) $-2C/3$ is the so-called deformation potential, that is, the energy change of the band bottom (or the top) due to unit dilation of lattice. M and v_0 denote the mass and the volume of a unit cell, κ and κ_0 are static and optical dielectric constants. u is an average sound velocity and $\omega/2\pi$ is the frequency of optical vibration, both referring to longitudinal waves. Ansel'm and Firsov[11] used (2·17) for the calculation of the mean free path of an exciton, confining themselves to the case $\lambda \neq \lambda' (=1s\text{-state})$, that is, to the *intra* band scattering, whereas Haken[10] took into account the *inter*band term $\lambda \neq \lambda'$ for the calculation of the self-energy of an exciton. Note that we can use (2·17) with (2·14), even when $\boldsymbol{k}_c \neq \boldsymbol{k}_v \neq 0$.

$q(\boldsymbol{w})$ in (2·14) is the Fourier transform of the charge distributions of the electron or the hole in the internal motion, because $p_e \cdot \boldsymbol{l}$, for instance, is the electron coordinate relative to the center of mass. It represents the effectivity of the electron or hole charge for a particular phonon $\boldsymbol{w}$. Now, $q(\boldsymbol{w}, \lambda\lambda')$ tends to unity or zero as w tends to zero, according as $\lambda = \lambda'$ or $\lambda \neq \lambda'$, while, in any case, it becomes very small when the wave length $2\pi/w$ of the phonon is smaller than the radius of the exciton, that is, the mean distance between the electron and the hole. For example, in the case of the $1s$-state of the relative motion with decay constant α, we have

$$q_e(\boldsymbol{w}\,;\, 1s1s) = \{1 + (p_e w/2\alpha)^2\}^{-2}. \tag{2·18}$$

(2·17) tells us that the optical mode is probably less important than the acoustic mode for the *intra*band scattering of an exciton, for $\beta_{op}(\boldsymbol{w})$ tends to zero as w when $\boldsymbol{w}$ tends to zero, whereas $\beta_{ac}(\boldsymbol{w})$ tends to zero as $w^{1/2}$; further it is in contrast with $\beta_{op}(\boldsymbol{w}) \propto w^{-1}$ for the case of a single electron. To the *inter*band scattering, however, both modes would make comparable contributions, because only the phonons with finite w would play a rôle in this case, due to the energy conservation.

§ 3. A general formula for the absorption coefficient

The Hamiltonian for the electron-lattice system is written as

$$H = H_e + H_L + H_{eL}, \tag{3·1}$$

where H_e, H_L and H_{eL} are given by (2·15) and (2·16). We now derive the coefficient of the optical absorption of this system which corresponds to the creation of an exciton.

Consider a radiation field R in the crystal medium which is assumed to be isotropic with refractive index n. Its Hamiltonian is given by

$$H_R = \sum_{\sigma,\boldsymbol{K}} \hbar\omega_{\boldsymbol{K}}\, c_{\sigma\boldsymbol{K}}{}^* c_{\sigma\boldsymbol{K}}, \quad \omega_{\boldsymbol{K}} = (c/n)K, \tag{3·2}$$

where $\sigma (=1, 2)$ and $\boldsymbol{K}$ refer to the polarization (the directions being denoted by unit vectors $\boldsymbol{e}_{\sigma\boldsymbol{K}}$) and wave-number of the photon, and $c^*_{\sigma\boldsymbol{K}}$ and $c_{\sigma\boldsymbol{K}}$ mean the creation-annihilation operators. c is the light velocity in vacuum. Strictly speaking, n is not constant in the frequency range we are considering; on the contrary, the absorption itself contributes to the dispersion of n. The most satisfactory way would be to determine n and absorption

ccefficient self-consistently. To avoid this rather complicated problem of dispersion relation, we take n to be constant over a range of frequency and equal to an appropriate average value.

It is sufficient, for the present purpose, to take into account the interaction of R with the electron system alone, H_{eR}, because in the frequency range at issue ($\omega \sim 10^{16}$ sec^{-1}), the vibration of lattice cannot follow that of the radiation field. Thus the total Hamiltonian is written as

$$H_{\mathrm{tot}} = H + H_R + H_{eR}. \tag{3·3}$$

Denoting the number of $(\sigma \boldsymbol{K})$-photons by $m_{\sigma K}$, the matrix element of H_{eR} which corresponds to the absorption of a $(\sigma \boldsymbol{K})$-photon with simultaneous creation of a $(\lambda \boldsymbol{K})$-exciton is calculated as

$$\begin{aligned}&(\Psi_{\lambda K}; \cdots, m_{\sigma K}-1, \cdots |H_{eR}| \Psi_0; \cdots, m_{\sigma K}, \cdots)\\ &= ie\hbar/mc\,(2\pi\hbar c m_{\sigma K}/v_0 nK)^{1/2}(\boldsymbol{e}_{\sigma K}\cdot \boldsymbol{g}_{\lambda K}),\end{aligned} \tag{3·4}$$

where

$$\begin{aligned}\boldsymbol{g}_{\lambda K} &\equiv N^{-1/2}\int\cdots\int \Psi_{\lambda K}^{*}\sum_{i=1}^{N}\nabla_i e^{i\boldsymbol{K}\boldsymbol{x}_i}\Psi_0 d\boldsymbol{x}_1\cdots d\boldsymbol{x}_N\\ &= \sum_{l} U_{\lambda K}^{*}(\boldsymbol{l})\int a_c^{*}(\boldsymbol{x}, \boldsymbol{l})\nabla e^{i\boldsymbol{K}\boldsymbol{x}} a_v(\boldsymbol{x}, 0)\, d\boldsymbol{x}.\end{aligned} \tag{3·5}$$

Let us now assume that initially the electron system is in the ground state Ψ_0 (no exciton), the lattice system in state Φ_n and the radiation field in state X_m. At the time T, the wave function of the total system is given by

$$\begin{aligned}&e^{-iH_{\mathrm{tot}}T/\hbar}\Psi_0\Phi_n X_m\\ &= e^{-i(H+H_R)T/\hbar}\Big[1 - i/\hbar\int_0^T e^{i(H+H_R)t_1/\hbar}H_{eR}e^{-i(H+H_R)t_1/\hbar}dt_1 + \cdots\cdots\Big]\Psi_0\Phi_n X_m.\end{aligned} \tag{3·6}$$

In the lowest order of perturbation, let us take, out of (3·6), the term corresponding to the state in which a $(\sigma \boldsymbol{K})$-photon is absorbed and an exciton (with any λ) is created:

$$\begin{aligned}&e/mc\cdot(2\pi\hbar c m_{\sigma K}/v_0 nK)^{1/2}e^{-i(m_{\sigma K}-1)\omega_{\sigma K}T}\sum_{\lambda}(\boldsymbol{e}_{\sigma K}\cdot\boldsymbol{g}_{\lambda K})\\ &\times\int_0^T e^{-i\omega_{\sigma K}t_1}e^{-iH(T-t_1)/\hbar}\Psi_{\lambda K}e^{-iH_L t_1/\hbar}\Phi\, dt_1 X_{\ldots, m_{\sigma K}-1, \ldots}\end{aligned} \tag{3·7}$$

Taking the absolute square of (3·7), and averaging over the initial distribution $n = (\cdots, n_w, \cdots)$ of vibrational states, we have, as the probability for that state to be realized,

$$W(m_{\sigma K},\ T)=(e/mc)^2\,2\pi\hbar c m_{\sigma K}/v_0 nK\cdot\sum_{\lambda}\sum_{\lambda'}(\boldsymbol{e}_{\sigma K}\cdot\boldsymbol{g}_{\lambda K}{}^*)\,(\boldsymbol{e}_{\sigma K}\cdot\boldsymbol{g}_{\lambda' K})$$
$$\times\int_0^T dt_1\int_{-t_1}^{T-t_1}dt\,e^{i\omega_{\sigma K}t}\{(\lambda\boldsymbol{K}|e^{-iHt/\hbar}|\lambda'\boldsymbol{K})\,e^{iH_L t/\hbar}\}_{Av}. \tag{3·8}$$

Here

$$\{\cdots\}_{Av}\equiv \mathrm{Tr}_L[e^{-\beta H_L}\{\cdots\}]/\mathrm{Tr}_L(e^{-\beta H_L}), \tag{3·9}$$

Tr_L referring to the lattice system alone, and $(\kappa\beta)^{-1}$ being the absolute temperature.

When T is large enough in (3·8), most of the contributions to $\int_0^T dt_1$ come from large values of t_1 and $T-t_1$, so that we can replace the upper and lower bound of the second integration by $\pm\infty$. Dividing by $Tm_{\sigma K}$, the lifetime τ of $(\sigma\boldsymbol{K})$-photon is given by

$$1/\tau(\sigma\boldsymbol{K})=(e/mc)^2\,2\pi\hbar c^2/v_0 n^2\omega_{\sigma K}\cdot\sum_{\lambda}\sum_{\lambda'}(\boldsymbol{e}_{\sigma K}\cdot\boldsymbol{g}_{\lambda K}{}^*)\,(\boldsymbol{e}_{\sigma K}\cdot\boldsymbol{g}_{\lambda' K})$$
$$\times\int_{-\infty}^{+\infty}dt\,e^{i\omega_{\sigma K}t}\{(\lambda\boldsymbol{K}|e^{-iHt/\hbar}|\lambda'\boldsymbol{K})\,e^{iH_L t/\hbar}\}_{Av}. \tag{3·10}$$

The absorption coefficient is defined as the reciprocal of penetration depth for which the radiation attenuates to e^{-1}. It is given, for the frequency $\omega=cK/n$, by

$$A(\omega)=n/c\cdot 1/2\cdot\sum_{\sigma}1/\tau(\sigma,\ \boldsymbol{K}), \tag{3·11}$$

where average was taken for the two directions of polarization.

(3·10) is nothing but the method of generating function (or the method of Fourier transform) which was applied to the radiative and non-radiative transitions of a trapped electron.[17),18)] In the present case, however, we cannot generally use the adiabatic approximation for the electron-lattice system H, because the exciton energy levels constitute continuous spectra due to the translational motion. We proceed in another way, and expand the exponential in (3·10) :

$$e^{-iHt/\hbar}=e^{-i(H_e+H_L)t/\hbar}\sum_{n=0}^{\infty}(i\hbar)^{-n}\int_0^t dt_1\cdots\int_0^{t_{n-1}}dt_n\cdot H'(t_1)\cdots H'(t_n), \tag{3·12}$$

where

$$H'(t)\equiv e^{i(H_e+H_L)t/\hbar}H_{eL}\,e^{-i(H_e+H_L)t/\hbar}$$
$$=i\sum_{\mu}\sum_{\lambda\lambda'}\sum_{\boldsymbol{K}\boldsymbol{w}}\beta_{\mu\lambda\lambda'}(\boldsymbol{w})\,e^{i(\varepsilon_{\lambda K+w}-\varepsilon_{\lambda' K})t/\hbar}$$
$$\times a^*_{\lambda K+w}a_{\lambda' K}(b_{\mu w}e^{-i\omega_{\mu w}t}-b^*_{\mu,-w}e^{i\omega_{\mu w}t}). \tag{3·13}$$

Defining

$$F_{\lambda\lambda'}(\boldsymbol{K})\equiv 1/2\cdot\sum_{\sigma}(\boldsymbol{e}_{\sigma K}\cdot\boldsymbol{g}_{\lambda K}{}^*)\,(\boldsymbol{e}_{\sigma K}\cdot\boldsymbol{g}_{\lambda' K}), \tag{3·14}$$

we have an infinite series expression for the absorption coefficient:

$$A(\omega)=2\pi\hbar e^2/m^2 v_0 cn\omega_{\boldsymbol{K}}\cdot\sum_{\lambda}\sum_{\lambda'}F_{\lambda\lambda'}(\boldsymbol{K})$$
$$\times\int_{-\infty}^{+\infty}dt\, e^{i\omega t-i\varepsilon_{\lambda\boldsymbol{K}}t/\hbar}\sum_{n}U_n(t\,;\,\lambda\lambda'\,;\,\boldsymbol{K}), \tag{3·15}$$

where

$$U_n(t\,;\,\lambda\lambda'\,;\,\boldsymbol{K})=(i\hbar)^{-n}\int_0^t dt_1\cdots\int_0^{t_{n-1}}dt_n(\lambda\boldsymbol{K}|H'(t_1)\cdots H'(t_n)\,|\lambda'\boldsymbol{K})_{Av}. \tag{3·16}$$

As $H'(t)$ of (3·13) is linear in the lattice co-ordinates $b_{\mu w}$ and $b_{\mu w}{}^*$, U_n vanishes for odd n. The first two terms are given by

$$U_0(t\,;\,\lambda\lambda'\,;\,\boldsymbol{K})=\delta_{\lambda\lambda'}, \tag{3·17}$$

$$U_2(t\,;\,\lambda\lambda'\,;\,\boldsymbol{K})=-\hbar^{-2}\int_0^t d\tau\int_\tau^t dt_1\sum_{\mu}\sum_{\lambda_1}\sum_{\boldsymbol{w}}\beta_{\mu\lambda\lambda_1}(-\boldsymbol{w})$$
$$\times\beta_{\mu\lambda_1\lambda'}(\boldsymbol{w})\,e^{i(\varepsilon_{\lambda\boldsymbol{K}}-\varepsilon_{\lambda'\boldsymbol{K}})t_1/\hbar}\,e^{i(\varepsilon_{\lambda'\boldsymbol{K}}-\varepsilon_{\lambda_1\boldsymbol{K}+\boldsymbol{w}})\tau/\hbar}$$
$$\times\{(n_{\mu w}+1)\,e^{-i\omega_{\mu w}\tau}+n_{\mu w}\,e^{i\omega_{\mu w}\tau}\}. \tag{3·18}$$

The diagonal ($\lambda=\lambda'$) term is further reduced to

$$U_2(t\,;\,\lambda\lambda\,;\,\boldsymbol{K})=-\hbar^{-2}\int_0^t(t-\tau)\,d\tau\sum_{\mu}\sum_{\lambda_1}\sum_{\boldsymbol{w}}|\beta_{\mu\lambda_1\lambda}(\boldsymbol{w})|^2$$
$$\times e^{i(\varepsilon_{\lambda\boldsymbol{K}}-\varepsilon_{\lambda_1\boldsymbol{K}+\boldsymbol{w}})\tau/\hbar}\{(n_{\mu w}+1)\,e^{-i\omega_{\mu w}\tau}+n_{\mu w}\,e^{+i\omega_{\mu w}\tau}\} \tag{3·19}$$
$$=-\hbar^{-2}\int_0^t d\tau\int_{-\infty}^{+\infty}dE(t-\tau)\,e^{-iE\tau/\hbar}f_{\lambda\boldsymbol{K}}(E), \tag{3·19′}$$

where

$$f_{\lambda\boldsymbol{K}}(E)\equiv\sum_{\mu}\sum_{\lambda_1}\sum_{\boldsymbol{w}}|\beta_{\mu\lambda_1\lambda}(\boldsymbol{w})|^2\{(n_{\mu w}+1)\,\delta(\varepsilon_{\lambda_1\boldsymbol{K}+\boldsymbol{w}}+\hbar\omega_{\mu w}-\varepsilon_{\lambda\boldsymbol{K}}-E)$$
$$+n_{\mu w}\,\delta(\varepsilon_{\lambda_1\boldsymbol{K}+\boldsymbol{w}}-\hbar\omega_{\mu w}-\varepsilon_{\lambda\boldsymbol{K}}-E)\}. \tag{3·20}$$

§ 4. The weak coupling limit

Consider a continuous function $f(E)$, the value of which is assumed not to vary appreciably over the range ΔE, or more specifically, $|f'(E)\,\Delta E|\lesssim f(E)$, that is:

$$\hbar/\Delta E\gtrsim\tau_c(E)\equiv\hbar f'(E)/f(E). \tag{4·1}$$

For a value of $|t|$ much larger than τ_c, we have an asymptotic formula[19]

$$\hbar^{-1}\int_0^t d\tau\int e^{-iE\tau/\hbar}f(E)\,dE\sim\int\{\pm\pi\delta(E)\;-i\mathscr{P}(1/E)\}f(E)\,dE\quad(|t|\gg\tau c), \tag{4·2}$$

where $\pm$ correspond to $t \lessgtr 0$. Thus (3·19′) becomes

$$U_2(t\,;\,\lambda\lambda\,;\,\boldsymbol{K}) = -\hbar^{-2}\int_0^t d\tau \int_{-\infty}^{+\infty} dE\, e^{-iE\tau/\hbar}(t+i\hbar\,\partial/\partial E)\cdot f_{\lambda\boldsymbol{K}}(E)$$

$$= -\mathscr{P}\int f'_{\lambda\boldsymbol{K}}(E)/E\cdot dE \mp i\pi f'_{\lambda\boldsymbol{K}}(0) - (\Gamma_{\lambda\boldsymbol{K}}/2)\,|t| - it\Delta_{\lambda\boldsymbol{K}}/\hbar, \qquad (4\cdot3)$$

where

$$\Gamma_{\lambda\boldsymbol{K}} \equiv (2\pi/\hbar) f_{\lambda\boldsymbol{K}}(0) = (2\pi/\hbar)\sum_{\mu}\sum_{\lambda_1}\sum_{\boldsymbol{w}} |\beta_{\mu\lambda_1\lambda}(\boldsymbol{w})|^2$$
$$\times\{(n_{\mu\boldsymbol{w}}+1)\,\delta(\varepsilon_{\lambda\boldsymbol{K}}-\varepsilon_{\lambda_1\boldsymbol{K}+\boldsymbol{w}}-\hbar\omega_{\mu\boldsymbol{w}})$$
$$+n_{\mu\boldsymbol{w}}\,\delta(\varepsilon_{\lambda\boldsymbol{K}}-\varepsilon_{\lambda_1\boldsymbol{K}+\boldsymbol{w}}+\hbar\omega_{\mu\boldsymbol{w}})\}, \qquad (4\cdot4)$$

$$\Delta_{\lambda\boldsymbol{K}} \equiv -\mathscr{P}\int f(E)/E\cdot\, dE = \sum_{\mu}\sum_{\lambda_1}\sum_{\boldsymbol{w}} |\beta_{\mu\lambda_1\lambda}(\boldsymbol{w})|^2$$

$$\times\left\{(n_{\mu\boldsymbol{w}}+1)\,\frac{\mathscr{P}}{\varepsilon_{\lambda\boldsymbol{K}}-\varepsilon_{\lambda_1\boldsymbol{K}+\boldsymbol{w}}-\hbar\omega_{\mu\boldsymbol{w}}} + n_{\mu\boldsymbol{w}}\,\frac{\mathscr{P}}{\varepsilon_{\lambda\boldsymbol{K}}-\varepsilon_{\lambda_1\boldsymbol{K}+\boldsymbol{w}}+\hbar\omega_{\mu\boldsymbol{w}}}\right\} \qquad (4\cdot5)$$

are the probability (per unit time) of the scattering, and the self-energy, of the $(\lambda\boldsymbol{K})$-exciton due to lattice vibration. $\delta(E)$ is Dirac's delta function and $\mathscr{P}$ means the principal value. Owing to $|t| \gg \tau_c$, the first two terms of (4·3) are small compared with the remaining terms; we therefore neglect the former for the present.

For the ultraviolet and visible regions of radiation, the photon wave number $\boldsymbol{K}$ is much smaller ($\sim 10^6$ cm^{-1}) than the reciprocal lattice vector ($\sim 10^8$ cm^{-1}), so that we can put $\boldsymbol{K}=0$ in the above.

If we take into account only the diagonal term $\lambda=\lambda'$ in (3·15), and approximate as

$$U_0(t\,;\,\lambda\lambda\,;\,0) + U_2(t\,;\,\lambda\lambda\,;\,0) + \cdots$$
$$= 1 + \{-(\Gamma_{\lambda 0}/2)\,|t| - it\Delta_{\lambda 0}/\hbar\} + \cdots \approx \exp\{-(\Gamma_{\lambda 0}/2)\,|t| - it\Delta_{\lambda 0}/\hbar\}, \qquad (4\cdot6)$$

we have, for the contribution of λ-exciton band to the absorption coefficient (3·15),

$$A_\lambda(\omega) = \frac{4\pi}{3}\,\frac{\hbar^2 e^2 |\boldsymbol{g}_{\lambda 0}|^2}{m^2 v_0 cn\omega}\,\frac{(\hbar\Gamma_{\lambda 0}/2)}{\{\hbar\omega - (\varepsilon_{\lambda 0}+\Delta_{\lambda 0})\}^2 + (\hbar\Gamma_{\lambda 0}/2)^2}. \qquad (4\cdot7)$$

(4·7) shows that the absorption band is of a Lorentzian shape, with a peak at $\varepsilon_{\lambda 0}+\Delta_{\lambda 0}$ and a half-value width $H=\hbar\Gamma_{\lambda 0}$ (if $\Gamma_{\lambda 0} \ll \omega$ as is always the case). The latter is nothing but the broadening of $(\lambda 0)$-level due to lattice scattering. Each absorption peak λ is expected to be free from the influence of other peaks if $\delta_{\lambda\lambda'} \equiv |\varepsilon_{\lambda 0} - \varepsilon_{\lambda' 0}| \gg \hbar\Gamma_{\lambda 0}$ and if the contribution of *inter*band terms $U_n(t\,;\,\lambda\lambda'\,;\,0)$ is negligible. The latter effect will be shown, in § 6, to be small if $\delta\hbar \gg \Gamma,\ \Delta$.

Of course, our approximation fails if, for values of $|t|$ satisfying $|t| \gtrsim \tau_c$, the exponential of (4·6) already decays to values much smaller than unity. Thus our approximation is valid only when $\Gamma_{\lambda 0}$ is so small that the condition

$$\Gamma_{\lambda 0}\tau_c/2 \ll 1 \tag{4·8}$$

is satisfied, in other words, when the exciton-lattice interaction is sufficiently weak. The more explicit form of the condition will be given in § 7. In any case, at the weak coupling limit, each of $U_{2m}(t\,;\,\lambda\lambda\,;\,0)$ $(m=0,\,1,\,2,\,\cdots)$ reduces to simpler form, leading to*

$$\sum_{m=0}^{\infty} U_{2m}(t\,;\,\lambda\lambda\,;\,0) = \sum_{m=0}^{\infty} \{-(\Gamma_{\lambda 0}/2)\,|t| - it\Delta_{\lambda 0}/\hbar\}^m/m!$$
$$= \exp\{-(\Gamma_{\lambda 0}/2)\,|t| - it\Delta_{\lambda 0}/\hbar\}. \tag{4·9}$$

Thus the approximation (4·6) proves to be exact in this limit.

Next we investigate the effect of the first two terms of (4·3). In the first approximation, we have, instead of (4·6),

$$U_0+U_2+\cdots \approx \{1-\mathscr{P}\int f'(E)/E\cdot dE\}\,\{1 \mp i\pi f'(0)\}$$
$$\times \exp\{-(\Gamma_{\lambda 0}/2)\,|t| - it\Delta_{\lambda 0}/\hbar\}. \tag{4·10}$$

Correspondingly, the Lorentzian function (the last factor of (4·7)) is replaced by

$$(1+\eta_\lambda)\,\frac{(\hbar\Gamma_{\lambda 0}/2)+2\mathscr{A}_\lambda\{\hbar\omega-(\varepsilon_{\lambda 0}+\Delta_{\lambda 0})\}}{\{\hbar\omega-(\varepsilon_{\lambda 0}+\Delta_{\lambda 0})\}^2+(\hbar\Gamma_{\lambda 0}/2)^2}, \tag{4·11}$$

where

$$\eta_\lambda = -\mathscr{P}\int f'(E)/E\cdot dE, \tag{4·12}$$

$$\mathscr{A}_\lambda = (\pi/2)f'(0). \tag{4·13}$$

The line shape of (4·11) is asymmetric: the peak position is given by $\hbar\omega_{\max}=(\varepsilon_{\lambda 0}+\Delta_{\lambda 0})+\frac{1}{2}\mathscr{A}_\lambda\hbar\Gamma_{\lambda 0}$, the half-value position on the high energy side by $\hbar\omega_{+1/2}=(\varepsilon_{\lambda 0}+\Delta_{\lambda 0})+(\frac{1}{2}+\mathscr{A}_\lambda)\hbar\Gamma_{\lambda 0}$, and that on the low energy side by $\hbar\omega_{-1/2}=(\varepsilon_{\lambda 0}+\Delta_{\lambda 0})-(\frac{1}{2}-\mathscr{A}_\lambda)\hbar\Gamma_{\lambda 0}$. The degree of asymmetry is thus given by

$$\{(\hbar\omega_{+1/2}+\hbar\omega_{-1/2})-2\hbar\omega_{\max}\}/\hbar\Gamma_{\lambda 0}=\mathscr{A}_\lambda. \tag{4·14}$$

In the first approximation as regards $f(E)$, the half-value width is not altered** whereas the peak height suffers the fractional change η_λ. As the total area of the λ-peak conserves so far as we neglect the non-diagonal $U(t\,;\,\lambda\lambda')$ $(\lambda'\neq\lambda)$, the compensating change must occur in the tail part of the absorption band.

§ 5. The strong coupling limit

If one takes the approximation of narrow exciton energy bands, whose exact meaning

---

* As for the proof of this theorem, see, for example, a work by van Hove.[20]

** Strictly speaking, $\Gamma_{\lambda 0}$ in the exponential function of (4·10) suffers the fractional change of the first order in $f(E)$, when one takes U_4 into account. However, so far as the product of the peak height and the half-value width is concerned, as will be in § 7, η_λ alone is effective for the change.

will be explained later, it is appropriate to expand $\exp\{i(\varepsilon_{\lambda K}-\varepsilon_{\lambda_1 K+w}\mp\hbar\omega_{\mu w})\tau/\hbar\}$ of (3·19) in a power series of τ when $\lambda_1=\lambda$, though it is not the case for $\lambda_1\neq\lambda$. Thus we have

$$U_2(t;\lambda\lambda;\boldsymbol{K})\dagger$$
$$=-\hbar^{-2}\sum_{\lambda_1}\int_0^t(t-\tau)\,e^{i(\varepsilon_{\lambda K}-\varepsilon_{\lambda_1 K})\tau/\hbar}d\tau$$
$$\times[B_{\lambda_1,\lambda\lambda}+\sum_{n=1}^{\infty}(i\tau/\hbar)^n/n!\cdot B^{(n)}_{\lambda_1,\lambda\lambda K}], \tag{5·1}$$

where

$$\left.\begin{aligned}B^{(n)}_{\lambda_1,\lambda\lambda' K}&=\sum_{\mu}\sum_{w}\beta^{*}_{\mu\lambda_1\lambda}(\boldsymbol{w})\beta_{\mu\lambda_1\lambda'}(\boldsymbol{w})\\&\times\{(n_{\mu w}+1)(\varepsilon_{\lambda_1 K}-\varepsilon_{\lambda_1 K+w}-\hbar\omega_{\mu w})^n\\&+n_{\mu w}(\varepsilon_{\lambda_1 K}-\varepsilon_{\lambda_1 K+w}+\hbar\omega_{\mu w})^n\}=B^{(n)*}_{\lambda_1\lambda' K},\\B_{\lambda_1,\lambda\lambda'}&\equiv B^{(0)}_{\lambda_1,\lambda\lambda' K}\ \text{(independent of } \boldsymbol{K}).\end{aligned}\right\} \tag{5·2}$$

The ratios of successive coefficients, $B^{(n+1)}/B^{(n)}$, are of the order of $(b/2)$ where b is the breadth of each exciton energy band (phonon energies $\hbar\omega_{\mu w}$ being neglected).

Consider the term $\lambda_1=\lambda$ in (5·1):

$$-\frac{B_{\lambda,\lambda\lambda}}{2\hbar^2}t^2+\sum_{n=1}^{\infty}\frac{B^{(n)}_{\lambda,\lambda\lambda}}{(n+2)!}\left(\frac{it}{\hbar}\right)^{n+2}, \tag{5·3}$$

and define

$$D_\lambda{}^2=B_{\lambda,\lambda\lambda}. \tag{5·4}$$

For values of $|t|$, for which the first term of (5·3) is of the order of unity, the n-th term is of the order of $(b/2D)^{n-1}/(n+1)!$. Assuming $b/2\ll D$, which means that the exciton energy bands are narrow enough, or that the exciton-lattice interaction is strong enough (see (5·4) and (5·2)), let us approximate

$$U_0(t;\lambda\lambda;\boldsymbol{K})+U_2(t;\lambda\lambda;\boldsymbol{K})_{\lambda_1=\lambda\text{only}}+\cdots$$
$$=1-\frac{D_\lambda{}^2}{2\hbar^2}t^2+\cdots\approx\exp\left(-\frac{D_\lambda{}^2}{2\hbar^2}t^2\right). \tag{5·5}$$

After Fourier transformation, we get the absorption coefficient for the λ-th band:

$$A_\lambda(\omega)=\frac{4\pi}{3}\frac{\hbar^2e^2|\boldsymbol{g}_{\lambda 0}|^2}{m^2v_0cn\omega}\frac{1}{\sqrt{\pi}D_\lambda}\exp\left\{-\frac{(\hbar\omega-\varepsilon_{\lambda 0})^2}{2D_\lambda{}^2}\right\}, \tag{5·6}$$

which is of a Gaussian shape with a peak at $\varepsilon_{\lambda 0}$ and a half-value width $H=2\sqrt{2(\ln 2)}D_\lambda$. (We have replaced $\varepsilon_{\lambda K}$ in (3·15) by $\varepsilon_{\lambda 0}$, because $D\gg b/2$.)

† Here we do not take $\boldsymbol{K}=0$, because, for the X-ray exciton which is one of the typical cases of strong coupling, $\boldsymbol{K}$ is not small.

The effects of $\lambda_1 \neq \lambda$ terms in (5·1), as well as those of non-diagonal $U_2(t\,;\,\lambda\lambda'\,;\,\boldsymbol{K})$ $(\lambda \neq \lambda')$, will be shown, in § 6, to be of secondary importance if we further assume that $\delta \gg D$, that is, the exciton energy bands are well separated from each other.

That we have taken out only the first term in (5·3) means that we have replaced $H'(t)$ in (3·16) by $H'(0)$. In this approximation, that is, in the limit

$$b/2 \ll D \ll \delta, \tag{5·7}$$

we can calculate all $U_{2m}(t\,;\,\lambda\lambda\,;\,\boldsymbol{K})$ $(m=0,\ 1,\ 2,\ \cdots)$ explicitly, with the result

$$\sum_{m=0}^{\infty} U_{2m}(t\,;\,\lambda\lambda\,;\,\boldsymbol{K}) = \sum_{m=0}^{\infty} \frac{1}{(2m)!}\left(\frac{-it}{\hbar}\right)^{2m}\left\{\frac{(2m)!}{2^m m!}\right\} D_\lambda^{2m}$$

$$= \exp\left(-\frac{D_\lambda^2}{2\hbar^2}t^2\right), \tag{5·8}$$

as is easily confirmed by considering the possible combinations of intermediate states in evaluating (3·16). Thus (5·5) proves to be exact in this limit.

That the generating function is written in a closed form (5·8) can be understood from another view-point. When the energy band is very narrow, the "localized exciton" is a sufficiently good eigenstate, and one can consider an adiabatic potential of lattice vibration for this localized exciton state. We can repeat the same mathematical manipulation as was done in the case of a trapped electron.[8] Thus, $H=H_e+H_L+H_{eL}$ is essentially the Hamiltonian for a harmonic oscillator system with equilibrium point displaced due to H_{eL}, the motion of the electronic system being practically freezed. Thus $\exp(-iHt/\hbar)$ in (3·10) can be calculated explicitly, leading to the same result as (5·8), provided phonon energies $\hbar\omega$ are neglected against D, as was done in deriving (5·8). The width D_λ of the absorption band is due to the difference in equilibrium positions of lattice before and after excitation.

§ 6. The effect of interband interaction

In the previous two sections we have neglected non-diagonal terms $U_n(t\,;\,\lambda\lambda'\,;\,\boldsymbol{K})$ $(\lambda \neq \lambda')$, and further, in the strong coupling case, the terms $\lambda_1 \neq \lambda$ in diagonal $U_n(t\,;\,\lambda\lambda\,;\,\boldsymbol{K})$. We now consider the effect of these terms on each absorption band λ.

In the weak coupling case, we proceed in the same way as in § 4. Making use of the formula (4·2), we have

$$U_2(t\,;\,\lambda\lambda'\,;\,0) = i\hbar\,(\varepsilon_{\lambda 0}-\varepsilon_{\lambda' 0})^{-1}\left[e^{i(\varepsilon_{\lambda 0}-\varepsilon_{\lambda' 0})t/\hbar}\left\{\pm\,(\Gamma^*_{\lambda'\lambda 0}/2)+i(\Delta^*_{\lambda'\lambda 0}/\hbar)\right\}\right.$$
$$\left.-\left\{\pm\,(\Gamma_{\lambda\lambda' 0}/2)+i(\Delta_{\lambda\lambda' 0}/\hbar)\right\}\right], \tag{6·1}$$

where $\pm$ depends on the sign of t, and $\Gamma_{\lambda\lambda' \boldsymbol{K}}$, $\Delta_{\lambda\lambda' \boldsymbol{K}}$ are defined as in (4·4) and (4·5), $|\beta_{\mu\lambda_1\lambda}(\boldsymbol{w})|^2$ being replaced by $\beta^*_{\mu\lambda_1\lambda}(\boldsymbol{w})\beta_{\mu\lambda_1\lambda'}(\boldsymbol{w})$. Multiplied with $\exp(-i\varepsilon_{\lambda 0}t/\hbar)$ apearing in (3·15), it is easy to see that the first term in (6·1) contributes to the λ'-peak, whereas the second to the λ-peak. Thus the contribution from

$$F_{\lambda\lambda'}(0)\, e^{-i\varepsilon_{\lambda 0}t/\hbar}\, U_2(t;\, \lambda\lambda';\, 0) + F_{\lambda'\lambda}(0)\, e^{-i\varepsilon_{\lambda' 0}t/\hbar}\, U_2(t;\, \lambda'\lambda;\, 0)$$

of (3·15) to the λ-peak becomes

$$-i\hbar(\varepsilon_\lambda - \varepsilon_{\lambda'})^{-1}\{\pm \mathrm{Re}\,(F_{\lambda\lambda'}\Gamma_{\lambda\lambda'}) + (2i/\hbar)\,\mathrm{Re}\,(F_{\lambda\lambda'}\Delta_{\lambda\lambda'})\}\, e^{-i\varepsilon_\lambda t/\hbar}, \qquad (6\cdot 2)$$

where the suffix $\boldsymbol{K}=0$ has been omitted for brevity.

Adding (6·2) to (4·6) as a correction term, we repeat the same procedure as used in the end of § 4. Finally we get the change of the peak height

$$\eta_\lambda = 2\sum_{\lambda'}{}' \mathrm{Re}\,(F_{\lambda\lambda'}\Delta_{\lambda\lambda'})/F_{\lambda\lambda}(\varepsilon_\lambda - \varepsilon_{\lambda'})\}, \qquad (6\cdot 3)$$

and the degree of asymmetry (the definition being given by (4·14))

$$\mathscr{A}_\lambda = (1/2)\sum_{\lambda'}\mathrm{Re}\,(F_{\lambda\lambda'}\hbar\Gamma_{\lambda\lambda'})/\{F_{\lambda\lambda}(\varepsilon_\lambda - \varepsilon_{\lambda'})\}, \qquad (6\cdot 4)$$

which are caused by the influence of other bands.

The effect of *inter*band interaction represented by η and $\mathscr{A}$ is small if $\delta_{\lambda\lambda'} \gg \Delta_{\lambda\lambda'}$, $\hbar\Gamma_{\lambda\lambda'}$, that is, if each energy band is well separated and the exciton-phonon interaction is sufficiently weak.

Let us now consider the strong coupling case. As in § 5, we calculate (3·18) or (3·19) by expanding $\exp\{i(\varepsilon_{\lambda_1 \boldsymbol{K}} - \varepsilon_{\lambda_1 \boldsymbol{K}+\boldsymbol{w}} \pm \hbar\omega_{\boldsymbol{w}})\tau/\hbar\}$ in power series, and take out the contribution to the λ-peak in the same way as is described in the above. The calculation being rather tedious, we only mention the result in the following.

Out of the summation

$$\sum_{\lambda'}\sum_{\lambda''} F_{\lambda'\lambda''}(\boldsymbol{K})\, e^{-i\varepsilon_{\lambda'\boldsymbol{K}}t/\hbar}\, U_2(t;\, \lambda'\lambda'';\, \boldsymbol{K}),$$

we take the terms which have $\exp(-i\varepsilon_{\lambda\boldsymbol{K}}t/\hbar)$ as a principal factor; the contribution to the coefficients from the non-diagonal part ($\lambda' \neq \lambda''$) is given by

$$\begin{aligned}
&\sum_{\lambda'}{}' \sum_{m=0}^{\infty} (\varepsilon_{\lambda'} - \varepsilon_\lambda)^{-(m+2)}\, 2\,\mathrm{Re}\,[F_{\lambda'\lambda}\{B^{(m)}_{\lambda',\lambda'\lambda} - (-1)^m B^{(m)}_{\lambda,\lambda'\lambda}\}] \\
&+ \sum_{\lambda'\neq\lambda''}{}' \sum_{m=0}^{\infty} (\varepsilon_{\lambda'} - \varepsilon_\lambda)^{-(m+1)}[(\varepsilon_{\lambda''} - \varepsilon_\lambda)^{-1} 2\,\mathrm{Re}\,(F_{\lambda''\lambda} B^{(m)}_{\lambda',\lambda''\lambda}) \\
&+ (-1)^n (\varepsilon_{\lambda''} - \varepsilon_{\lambda'})^{-1}\, 2\,\mathrm{Re}\,(F_{\lambda''\lambda'} B^{(m)}_{\lambda,\lambda''\lambda'})] \\
&+ \sum_{\lambda'}{}' \sum_{n=1}^{\infty} (it/\hbar)^n/n! \cdot \sum_{m=0}^{\infty} (-1)^m (\varepsilon_{\lambda'} - \varepsilon_\lambda)^{-(m+1)}\, 2\,\mathrm{Re}\,(F_{\lambda\lambda'} B^{(n-1+m)}_{\lambda,\lambda\lambda'}) \\
&+ \sum_{\lambda\neq\lambda''}{}' \sum_{n=1}^{\infty} (it/\hbar)^n/n! \cdot \sum_{m=0}^{\infty} (-1)^m \\
&\times (\varepsilon_{\lambda'} - \varepsilon_\lambda)^{-m} (\varepsilon_{\lambda'} - \varepsilon_{\lambda''})^{-1}\, 2\,\mathrm{Re}\,(F_{\lambda''\lambda'} B^{(n-1+m)}_{\lambda,\lambda''\lambda'}), \qquad (6\cdot 5)
\end{aligned}$$

while the contribution from the diagonal part is written as

$$\sum_{\lambda'}{}' F_{\lambda'\lambda'} \sum_{m=0}^{\infty} (-1)^m (m+1)\, (\varepsilon_{\lambda'} - \varepsilon_\lambda)^{-(m+2)} B^{(m)}_{\lambda,\lambda'\lambda'}$$

$$
\begin{aligned}
&- \sum_{\lambda\prime}{}' F_{\lambda\lambda} \sum_{m=0}^{\infty} (m+1)\,(\varepsilon_{\lambda\prime}-\varepsilon_{\lambda})^{-(m+2)} B^{(m)}_{\lambda\prime,\lambda\lambda} \\
&+ \sum_{\lambda\prime}{}' F_{\lambda\prime\lambda\prime}\,(it/\hbar) \sum_{m=0}^{\infty} (-1)^m (m+1)\,(\varepsilon_{\lambda\prime}-\varepsilon_{\lambda})^{-(m+2)} B^{(m+1)}_{\lambda,\lambda\prime\lambda\prime} \\
&+ \sum_{\lambda\prime}{}' F_{\lambda\lambda}\,(it/\hbar) \sum_{m=0}^{\infty} (\varepsilon_{\lambda\prime}-\varepsilon_{\lambda})^{-(m+1)} B^{(m)}_{\lambda\prime,\lambda\lambda} \\
&+ \sum_{\lambda\prime}{}' F_{\lambda\prime\lambda\prime} \sum_{n=2}^{\infty} (it/\hbar)^n/n! \cdot \sum_{m=0}^{\infty} (-1)^m (m+1)\,(\varepsilon_{\lambda\prime}-\varepsilon_{\lambda})^{-(m+2)} B^{(n+m)}_{\lambda,\lambda\prime\lambda\prime} \\
&+ F_{\lambda\lambda} \sum_{n=2}^{\infty} (it/\hbar)^n/n! \cdot B^{(n-2)}_{\lambda,\lambda\lambda}. \qquad (6\cdot6)
\end{aligned}
$$

Here the primed summation means that $\lambda'=\lambda$ or $\lambda''=\lambda$ is to be omitted.

The last term of (6·6) has been discussed in § 5. All the other terms of (6·6) and (6·5) represent the influence of other exciton bands. It is easy to see that these terms are small compared with the last term of (6·6) for values of $t \lesssim \hbar/D_{\lambda}$ (see (5·8)), if the condition (5·7) is satisfied. For instance, a typical term of the last line of (6·5) are smaller than the last term of (6·6) by the order of

$$(D/\delta)^{m+1}(b/2D)^{m+(n-1)} \quad (m \geqq 0,\ n \geqq 1).$$

Thus it is reasonable to regard (5·7) as a sufficient condition for the absorption band to be Gaussian and for the influence of other bands to be negligible, although a complete proof would require the considerations of $U_n(t;\lambda\lambda'\boldsymbol{K})$ with $n \geqq 4$.

The constant terms in (6·5) and (6·6) give the change of the strength (area) of the λ-peak, the terms proportional to $(it/\hbar)$ give the shift, and the terms with $(it/\hbar)^2$ are related with the change of the width, due to the influence of other exciton bands.

§ 7. Further discussions of the theoretical conclusions

In this section we rewrite the conclusions of the previous three sections more explicitly, by making use of appropriate models or approximations in calculating relevant quantities.

(i) *Calculation of $\Gamma_{\lambda K}$ in the effective mass approximation*

This quantity, given by (4·4), is not only related to the width of the absorption band in the weak coupling case, but it is also important in discussing the dynamical behavior of excitons in the vibrating lattice field. It consists of the *intra*band and *inter*band transitions, of which we here confine ourselves to the former.

Let us take the effective mass approximation (2·2) ~ (2·9), m_e and m_h being assumed to be isotropic. We take the lowest exciton band, and assume that the wave function for the relative motion is of a hydrogenic $1s$-type: $\varphi_{1s}(\boldsymbol{l}) = (\alpha^3/\pi)^{1/2} \exp(-\alpha l)$. Putting (2·16) (2·17) and (2·18) into (4·4), we get, as the contribution of the acoustical mode to the $1s \to 1s$ scattering (see also ref. 11),

$$\Gamma_{1s,\boldsymbol{K}\to 1s}(\text{ac.}) = \frac{4m^* v_0 \kappa T}{9\pi\hbar^3 Mu^2}(C_v - C_c)^2$$

$$\times \begin{cases} 2w_{ac} & (K^* < w_{ac} \text{—region } I), \qquad (7\cdot 1) \\ (K^{*2} + w_{ac}^2)/K^* & (w_{ac} < K^* \ll \alpha,\ w_0 \text{—region } II), \qquad (7\cdot 1') \end{cases}$$

$$= \frac{4m^* v_0 \kappa T}{9\pi\hbar^3 Mu^2} \frac{\alpha^2}{K^*}\left(\frac{C_v^2}{3p_h^2}\left\{1-\left(1+\frac{p_h^2 K^{*2}}{\alpha^2}\right)^{-3}\right\}\right.$$

$$+\frac{C_c^2}{3p_e^2}\left\{1-\left(1+\frac{p_e^2 K^{*2}}{\alpha^2}\right)^{-3}\right\} - \frac{2C_v C_c}{(p_h^2-p_e^2)^2}$$

$$\times\left[p_h^2\left\{1-\left(1+\frac{p_h^2 K^{*2}}{\alpha^2}\right)^{-1}\right\} + p_e^2\left\{1-\left(1+\frac{p_e^2 K^{*2}}{\alpha^2}\right)^{-1}\right\}\right.$$

$$\left.\left. - \frac{2p_h^2 p_e^2}{p_h^2-p_e^2}\log\left\{\frac{1+(p_h^2 K^{*2}/\alpha^2)}{1+(p_e^2 K^{*2}/\alpha^2)}\right\}\right]\right)$$

$$(w_{ac} \quad K^* \text{—region } III), \qquad (7\cdot 1'')$$

where

$$w_{ac} \equiv m^* u/\hbar \ll w_0, \qquad (7\cdot 2)$$

the former being of the order of $10^6\,\text{cm}^{-1}$ while the latter, the Debye cut-off wave-number, of the order of $10^8\,\text{cm}^{-1}$. $(7\cdot 1)\sim(7\cdot 1'')$ are plotted, as a function of

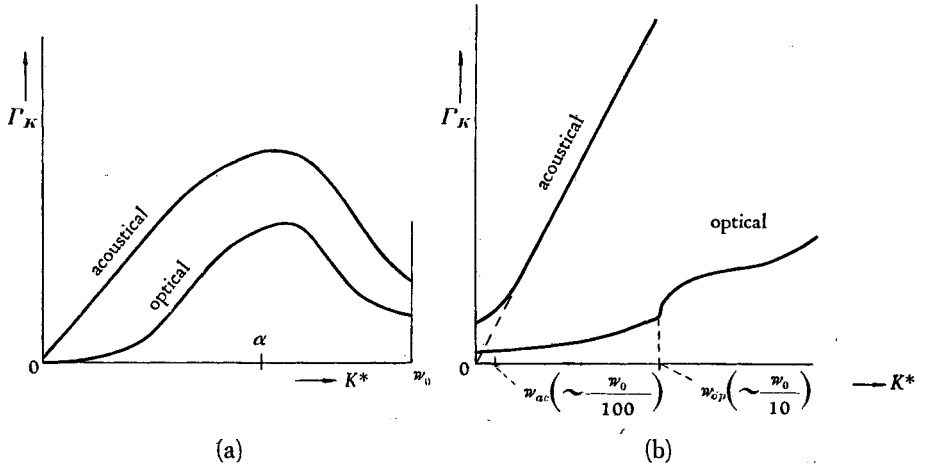

Fig. 2. The scattering probabilities Γ_K of an exciton with wave number $\boldsymbol{K}=\boldsymbol{K}_0+\boldsymbol{K}^*$, due to acoustical and optical modes, as functions of $\boldsymbol{K}^*$.

$\boldsymbol{K}^*(\equiv\boldsymbol{K}-\boldsymbol{K}_0)$, in Fig. 2. They are valid at high temperatures $T \gtrsim \Theta_0(\boldsymbol{K}^*)$, while at very low temperatures $T \ll \Theta_0(\boldsymbol{K}^*)$, T should be replaced by $\Theta_0(\boldsymbol{K}^*)$ in these formulae. Here the characteristic temperature $\Theta_0(\boldsymbol{K}^*)$ is given by

$$\Theta_0(\boldsymbol{K}^*) = (2\hbar u/3\kappa) \times \begin{cases} (3w_{ac}^2 + K^{*2})/w_{ac} & \text{(Region } I\text{)}, \quad (7\cdot3) \\ (K^* + w_{ac})^3/(K^{*2} + w_{ac}^2) & \text{(Region } II\text{)}, \quad (7\cdot3') \end{cases}$$

the expression for the region *III* being omitted as it is rather complicated. It is plotted in Fig. 3 for a typical case. It is of the order of $(\alpha/w_0)\,\Theta_D = \hbar u\alpha/\kappa$ when $K^* \sim w_0$.

In the case of the optical mode we get

$$\Gamma_{1s,\boldsymbol{K}\to 1s}(\text{op.}) = \omega e^2\left(\frac{1}{\kappa_0} - \frac{1}{\kappa}\right)\frac{1}{2}(p_h^2 - p_e^2)^2\frac{m^*}{\hbar^2\alpha^4}$$

$$\times \begin{cases} \bar{n}(2K^{*2} + w_{op}^2)\sqrt{K^{*2} + w_{op}^2} & (0 < K^* < w_{op} \text{— region } I'), \quad (7\cdot4) \\ [\bar{n}(2K^{*2} + w_{op}^2)\sqrt{K^{*2} + w_{op}^2} + (\bar{n}+1)(2K^{*2} - w_{op}^2)\sqrt{K^{*2} - w_{op}^2}] & \\ \qquad (w_{op} < K^* \ll \alpha,\ w_0 \text{— region } II'), \quad (7\cdot4') \end{cases}$$

where

$$w_{op} \equiv (2m^*\omega/\hbar)^{1/2} \ll w_0, \quad (7\cdot5)$$

the former being of the order of $10^7\ \text{cm}^{-1}$. The expression for the region *III'*: $K^* \gg w_{op}$ has been omitted for brevity (see also ref. 11). These are plotted in Fig. 2 for a typical case.

It is to be noted that for all values of $\boldsymbol{K}^*$ the contribution of the optical mode is relatively unimportant, as is already stated in § 2. Especially, for small values of K^*, the contribution is quite negligible compared with that of the acoustical mode (see Fig. 2a). Thus, a thermal exciton with $K^* \sim (3m^*\kappa T/\hbar^2)^{1/2}$ is scattered by acoustical vibrations alone. The mean free path l is given by

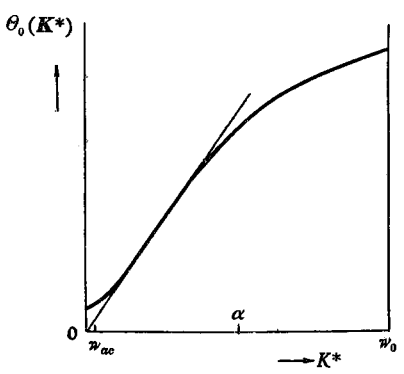

Fig. 3. The characteristic temperature $\Theta_0(\boldsymbol{K}^*)$ for $\Gamma_{1s\,K\to 1s}$ (ac).

$$l^{-1} = \Gamma(\hbar K^*/m^*)^{-1} = \frac{4}{9\pi}\frac{m^{*2}v_0\kappa T}{\hbar^4 M u^2}(C_v - C_c)^2, \quad (7\cdot6)$$

for values of K^* which are $\gg w_{ac}$ and $\ll \alpha$, w_0, being independent of K^*. It is valid at all temperatures, except at very low temperatures of a few degree (see (7·3')). Moreover, it does not depend on the wave function of the internal motion of the exciton.

In the same way, we can calculate $\Delta_{\lambda\boldsymbol{K}}$ and D_λ, which are related to the peak shift in the weak coupling case and to the half-value width in the strong coupling case, respectively; however the result is rather complicated, and will not be written here.

(ii) *A simplified approximation for the overall structure of* $f(E)$

The effective mass approximation used in the above has two drawbacks; firstly, it is valid only for the excitons near the extremum of the energy band; secondly it is presumably not a good approximation for the *internal* motion of the exciton which has a binding energy as large as 1∼2 eV, as is the case for alkali-halide crystals.

As regards the latter situation, it would be more practical, at least in the present stage, to take into account the effect of internal motion by assuming, in (2·17), that

$$q_e(\boldsymbol{w};\lambda\lambda)=q_h(\boldsymbol{w};\lambda\lambda)=\begin{cases}1 & \text{when } w<w_\lambda^{(e)},\\ 0 & \text{when } w_\lambda^{(e)}<w<w_0,\end{cases} \tag{7·7}$$

where $(w_\lambda^{(e)})^{-1}$ is of the order of exciton radius. Then the calculation of D_λ defined by (5·4) and (5·2) becomes quite simple, the result is written as*

$$D^2=\frac{4}{9}\frac{C^2}{Mu^2}\left(\frac{w^{(e)}}{w_0}\right)^3\times\begin{cases}\kappa T & T\gtrsim\Theta_0,\\ \kappa\Theta_0 & T\ll\Theta_0,\end{cases} \tag{7·8}$$

where

$$\Theta_0=(3/8)\hbar u w^{(e)}/\kappa, \tag{7·9}$$

and $C\equiv C_e-C_v$.

As for the first problem, we note that not the local (the neighborhood of the bottom or the top) but rather overall structure of the exciton energy band is important in calculating $f_\lambda(E)$, which was defined by (3·20) and characterizes the main feature of the line shape.

If we confine ourselves to *intra*band effect, and moreover neglect phonon energies in (3·20), $f_\lambda(E)$ is different from zero in the interval $(\varepsilon_{\lambda b}-\varepsilon_{\lambda 0},\ \varepsilon_{\lambda t}-\varepsilon_{\lambda 0})$, where $\varepsilon_{\lambda b}$ and $\varepsilon_{\lambda t}$ means the energies of the bottom and the top of the energy band. Further, it is easily confirmed that at the both ends of the interval $f(E)$ tends to zero as $\{E-(\varepsilon_{\lambda b}-\varepsilon_{\lambda 0})\}^{1/2}$ or $\{(\varepsilon_{\lambda t}-\varepsilon_{\lambda 0})-E\}^{1/2}$. If most part of the λ-energy band lies on the high energy side of $\varepsilon_{\lambda 0}$, it is rather plausible to suppose that the peak shift Δ is negative according to (4·5), and that the asymmetry $\mathscr{A}$ is positive due to (4·13).

In order to take into account these situations in a simplest way we assume the following functional form for $f(E)$:

$$f_\lambda(E)=\frac{s_\lambda}{\pi}\left\{\left(\frac{b_\lambda}{2}\right)^2-\left(E-\frac{b_\lambda}{2}p_\lambda\right)^2\right\}^{1/2}\quad(-1\leqq p_\lambda\leqq+1), \tag{7·10}$$

where b_λ is the breadth of the λ-energy band, and p_λ is a parameter representing the position of $\varepsilon_{\lambda 0}$ in the whole energy band. $p=+1(-1)$ corresponds to the case that $\boldsymbol{K}=0$ is at the bottom (top) of the band. The normalization constant s_λ is determined by considering that the integral of $f_\lambda(E)$ is equal to D_λ^2 according to (3·20) and (5·2) ; that is :

$$s_\lambda=8D_\lambda^2/b_\lambda^2. \tag{7·11}$$

Note that a large s corresponds to a *large* coupling constant, to *high* temperatures or to a *narrow* energy band, as is easily seen from (7·8) and (7·11). In the following, we shall omit the suffix λ so far as the *intra*band effect is concerned.

Making use of (7·10) we can calculate the quantities given by (4·4), (4·5), (4·12) and (4·13) ; the results are as follows :

$$H=\hbar\Gamma=s\sqrt{1-p^2}\,b, \tag{7·12}$$

$$\Delta=-(sp/2)\,b, \tag{7·13}$$

$$\mathscr{A}=(sp/2)/\sqrt{1-p^2}, \tag{7·14}$$

$$\eta=s. \tag{7·15}$$

(iii) *Criterion for the classification into Lorentzian and Gaussian cases*

The power series (5·1) is calculated, with the use of (7·10) and (7·11), as

$$U_2=-\frac{1}{2}D^2\left(\frac{t}{\hbar}\right)^2+\frac{1}{12}ipD^2b\left(\frac{t}{\hbar}\right)^3+\frac{1}{96}\left(p^2+\frac{1}{4}\right)D^2b^2\left(\frac{t}{\hbar}\right)^4+\cdots. \tag{7·16}$$

If $s\gg 1$, we can neglect all but the first term in (7·16), as well as in U_4, U_6, ···,

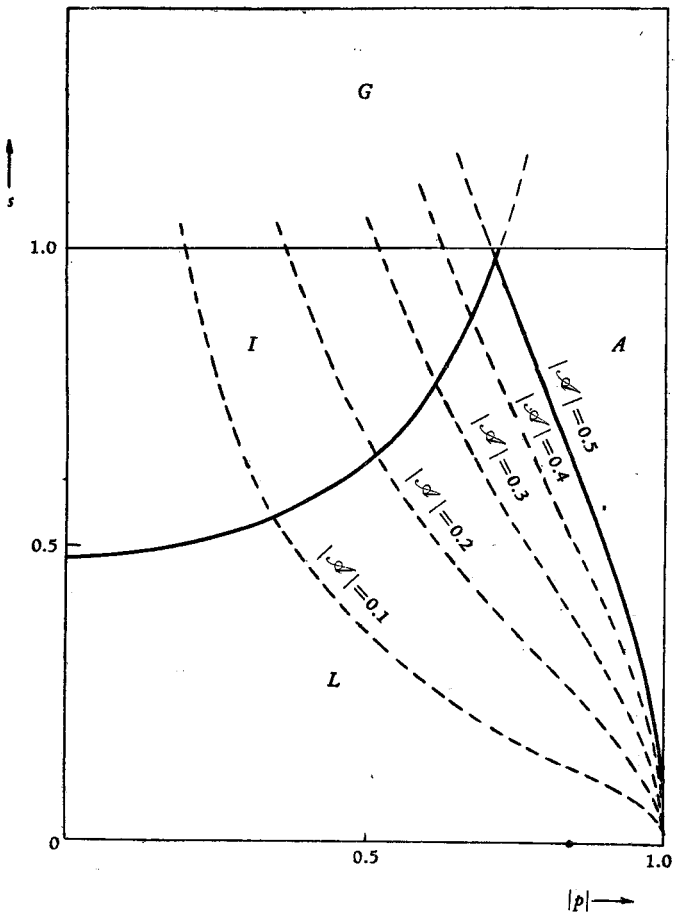

Fig. 4. The classification into Gaussian, Lorentzian, Asymmetric and Intermediate cases according to values of p and s.

and therefore get (5·8), which leads to a Gaussian line shape.

Next we introduce the ratio of the half-value width formula for the Lorentzian case to that for the Gaussian case :

$$r \equiv \frac{\hbar\Gamma_{\lambda 0}}{2\sqrt{2\,(\ln 2)\,D_\lambda}} = \frac{1}{\ln 2}\sqrt{1-p^2}\sqrt{s}. \tag{7·17}$$

According as $r \gg 1$ or $r \ll 1$, the *dynamical* region (5·5) or the *stochastic* region (4·6) becomes more important than the other. In order that the Lorentzian case is realized, not only the relation $r \ll 1$, but also (4·8) should be satisfied. In the present approximation, $\tau_c(0)$ defined by (4·1) is calculated as*

$$\tau_c(0) = \{2|p|/(1-p^2)\}\hbar/b, \tag{7·18}$$

and (4·8) is rewritten as follows :

$$s|p|/\sqrt{1-p^2} = 2|\mathscr{A}| \ll 1. \tag{7·19}$$

In Fig. 4 we divide the $(|p|, s)$ plane into several regions according to the above discussions. The region G (Gaussian) is defined by $s > 1$, whereas L (Lorentzian) is determined by $r < 1$ and $|\mathscr{A}| < 1/2$. We denote by A (asymmetric) the region where $s < 1$ and $|\mathscr{A}| > 1/2$, and the remaining region will be called I (intermediate).

(iv) *Temperature dependence and the effect of lattice imperfections.*

In the above discussions we have considered the dynamical vibrations of the lattice. When there are any types of lattice imperfections such as dislocations, vacancies, interstitial atoms or impurities, a static displacement of the lattice is brought about. The expectation values $\overline{b_{\mu w}^*}$, $\overline{b_{\mu w}}$ are generally not equal to zero. If, however, the imperfections are distributed at random, as is presumably the case in actual crystals, the linear effect of $\overline{b}$ almost cancels out, and we have only to replace $\overline{n_{\mu w}} = \overline{b_{\mu w}^* b_{\mu w}} \propto T\,(T \gtrsim \Theta_D)$ by a suitable quantity which is proportional to the density of imperfections. Thus the effect of increasing imperfections are qualitatively the same as

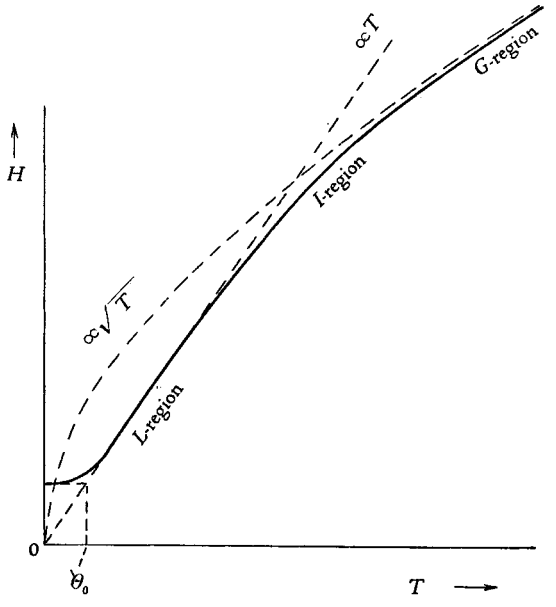

Fig. 5. A typical temperature dependence of the half-value width H expected from theory.

* We use $\tau_c(0)$ instead of $\tau_c(E)$, because the value near $E=0$ is the most important in using the δ-function approximation (4·2).

that of raising temperatures. In the following statements, which concern the *temperature* dependence of the line-shape, the word "absolute temperature" can be replaced, when one deals with the dependence on *imperfection*, by "the density of imperfections" with a suitable proportionality constant, without any other substantial modifications.

As we have seen in (iii), the exciton absorption band is of a Gaussian shape when the exciton-lattice coupling is strong or the exciton energy band is narrow (corresponding to large effective mass), while it is Lorentzian in the opposite limit. If these quantities are in suitable ranges, s increases from a value $s<1$ at $T=0°\mathrm{K}$ to values >1 at high temperatures (see (7·11) and (7·8)); that is, the line shape is Lorentzian at low temperatures and tends to Gaussian as the temperature is raised. If $\varepsilon_{\lambda 0}$ is near the bottom or the top of the energy band $(1-|p|\ll 1)$, the line shape is strongly asymmetric in a rather wide-spread intermediate range of s (see Fig. 4).

In the region L, the half-value width H is proportional to T except at low temperatures ($T \lesssim \theta_0$, see (7·12), (7·11) and (7·8)), while it is proportional to $\sqrt{T}$ in G (see Fig. 5).

The *inter*band interaction becomes important when other exciton energy bands lie close to the band we are considering. For example, the peak shift (being proportional to T) due to the *intra*band effect is given by (7·13), and it is negative or positive according as $\varepsilon_{\lambda 0}$ is near the bottom or the top of the band, while the contribution of the *inter*band effect is given by

$$\Delta_\lambda \approx \sum_{\lambda'}{}' \frac{B_{\lambda'\lambda,\lambda\lambda}}{\varepsilon_{\lambda 0}-\varepsilon_{\lambda' 0}} \sim O\left(\frac{D^2}{\delta}\right) \tag{7·20}$$

according to (4·5), which is negative for the lowest exciton band. In the region G, the contribution of *intra*band effect to the shift is small, whereas the *inter*band transition causes a shift given by

$$\Delta_\lambda' \approx \sum_{\lambda'}{}' \frac{1}{\varepsilon_{\lambda 0}-\varepsilon_{\lambda' 0}} \left\{B_{\lambda'\lambda,\lambda\lambda}+\frac{\mathrm{Re}\,(F_{\lambda'\lambda}B_{\lambda,\lambda'\lambda})}{F_{\lambda\lambda}}\right\} \sim O\left(\frac{D^2}{\delta}\right), \tag{7·21}$$

if we take the terms with the lowest order in (b/δ), out of the coefficients of $(-it/\hbar)$ in (6·5) and (6·6). In the same approximation the dispersion in the region G is given by

$$D_\lambda^2-\Delta_\lambda'^2. \tag{7·22}$$

The first term of (7·22) is proportional to T while the second is to T^2. It is possible that as temperature rises the half-value width tends to saturate or even to decrease, although in such regions, the peak separation becomes very poor due to $D\sim\delta$.

As for the asymmetry in the region L, there is a contribution from the *inter*band effect given by (6·4), besides the *intra*band effect (7·14). It is to be noted that both are proportional to T. If two exciton bands lie very close to each other, and if the *inter*band contribution is dominant as regards $\mathscr{A}$, both absorption peaks are expected to have slower decents towards the outside (Fig. 6a) or the inside (Fig. 6b) according as

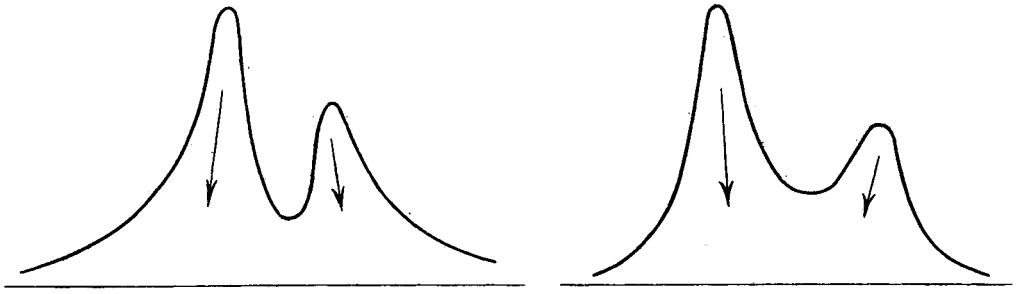

(a) $\mathrm{Re}(F_{\lambda\lambda'}\Gamma_{\lambda\lambda'})>0$ (b) $\mathrm{Re}(F_{\lambda\lambda'}\Gamma_{\lambda\lambda'})<0$

Fig. 6. The interband effect on the asymmetries of adjacent peaks.

$\mathrm{Re}(F_{\lambda\lambda'}\Gamma_{\lambda\lambda'})\lessgtr 0$, the smaller peak being distorted more strikingly than the larger one.

In the region L, the product of the peak height and the half-value width varies as $1+\eta$, where η is proportional to T (at $T\gtrsim\theta_0$). The contribution from the *intra*band transition is given by (7·15) and is positive,* whereas the *inter*band effect is given by (6·3). In the region G, η is mainly due to the *inter*band effect. In the lowest order of (b/δ), it is given by

$$\eta_\lambda=\sum_{\lambda'}{}'\frac{B_{\lambda',\lambda\lambda}}{(\varepsilon_{\lambda 0}-\varepsilon_{\lambda' 0})^2}\frac{-F_{\lambda\lambda}+F_{\lambda'\lambda'}}{F_{\lambda\lambda}}+\sum_{\lambda'}{}'\frac{2}{(\varepsilon_{\lambda 0}-\varepsilon_{\lambda' 0})^2}\frac{\mathrm{Re}\{F_{\lambda'\lambda}(B_{\lambda',\lambda'\lambda}-B_{\lambda,\lambda'\lambda})\}}{F_{\lambda\lambda}} \tag{7·23}$$

(see (6·5) and (6·6)), and is proportional to T.

(v) *Physical meanings of the criterion*

Let us consider the meaning of $\tau_c(0)$ defined by (4·1). According to (4·2) and (4·3), the probability that an exciton has suffered a collision by a phonon is proportional to t only if $|t|\gg\tau_c$. τ_c is considered to be a minimum duration time of collision: if we imagine a wave packet of an exciton which collides with a wave packet of a phonon and is then scattered, the collision duration time is of the order of τ_c in the most favorable cases (that is, for appropriate forms of the initial wave packets). Thus the condition (4·8) for the Lorentzian case means that the time between successive collisions is large compared with the collision duration. This is the well-known condition for the validity of the usual transport equations, and was discussed by Peierls[21] for the case of metallic conductivity, by Seitz[22] for the case of semiconductors, and has recently been extended to general case by van Hove.[20]

It is instructive to compare the division in Fig. 4 with the "polaron" problem.[16] The region L corresponds to the weak-coupling case, where the usual perturbation theoretical calculation is valid, while the region G corresponds to the strong coupling case where

* That it is positive seems to be very probable, *irrespective* of the approximation (7·10). For, in (4·12), $f'(E)$ is positive (negative) near the bottom (the top) of the band, where $\dot{E}$ is negative (positive).

the so-called self-trapped electron is a good approximation. The region A corresponds to a slow electron (note that $1-|p|\ll 1$) in the intermediate coupling case whose exact treatment is rather difficult. In our case, too, it would be necessary to take into account the cloud effect suitably, in order to discuss the line shape for the region A more elaborately.

The situation in the Lorentzian case is analogous to the motional or exchange narrowing effects of magnetic resonances.[23] Thus, excitation energy ($\varepsilon_{\lambda 0}$), kinetic energy of an exciton ($\varepsilon_{\lambda K}-\varepsilon_{\lambda 0}$) and exciton-lattice interaction H_{eL} of our case correspond to Zeeman energy, exchange coupling and dipolar interaction, respectively, of the magnetic case.

§ 8. Comparison with experimental results

We now compare the theoretical conclusions stated in the previous section with several experimental data available at present.

(i) Analysis of Fesefeldt's[24] and Martienssen's[25] data shows that at low and room temperatures, the first exciton absorption bands of KI and RbBr crystals are Lorentzian in the main, while it approaches the Gaussian shape at high temperatures, as is expected from theory (see § 7 (iv)). Other alkali-halides seem to show the same tendency, though not so clearly as in KI and RbBr.

According to Tutihasi's[26] data on AgCl crystal, the absorption curve on the low energy side of the first peak, at $T=-184\,^{\circ}\mathrm{C}$, is in excellent agreement with a Lorentzian curve, with half-value width $H=0.177$ eV. On the high energy side, overlaps with other bands prevent the analysis.

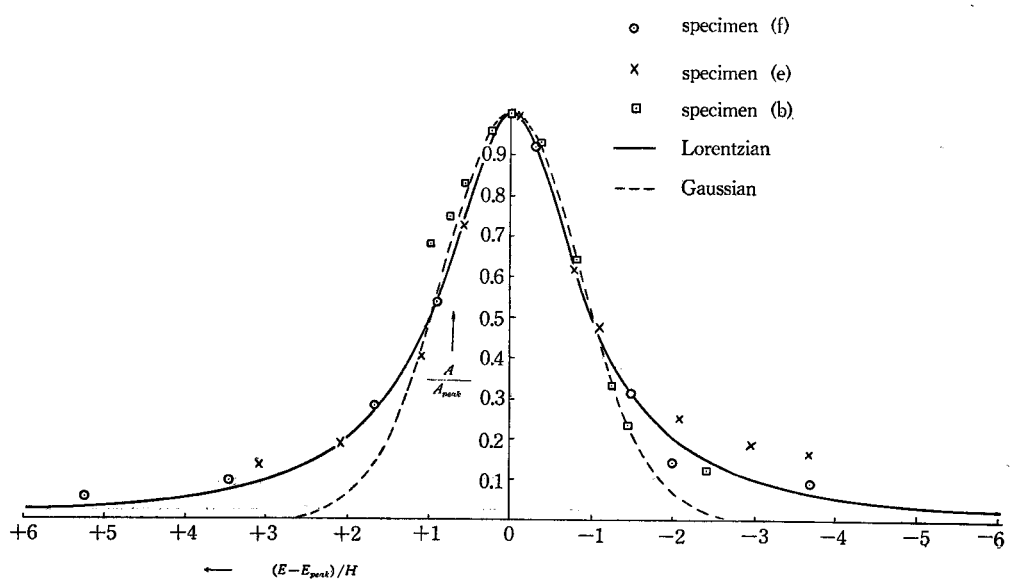

Fig. 7. The absorption curves for the first peak of KI (containing 10 mol % of KF) measured by Fischer. The peak height and the half-value width are reduced to unity for each specimen.

Table 1. The results of analysis of Fischer's data on the first absorption peak of KI crystals containing 10 mol % of KF.

specimen	peak position	peak height	half-value width H	line shape	asymmetry $\mathscr{A}$	area
(f)	5.844 eV	2.16	0.067 eV	L	very small	0.178
(e)	5.840	1.40	0.115	L	−0.08	0.198
(d)	5.795	0.674	0.37	(L)	−0.30	0.305
(c)	5.63					
(b)	5.51	0.467	0.42	G		0.196
(a)	5.48	0.434	0.40	G		0.174

Fischer[27] measured, at $T=20°K$, the absorption coefficients of a number of KI (containing 10 mol % of KF*) films with different preliminary heat treatments. The higher the temperature is maintained or the longer the treatment is continued, the less will be the crystal imperfections. In his specimens (f) and (e), which are considered to be the most perfect ones, the first peak is of a Lorentzian shape with relatively small width, while the specimen (b) and (a) which must have high densities of imperfections show nearly Gaussian shapes with large widths, as is shown in Fig. 7 and Tab. 1. These results again confirm the theoretical expectation (see § 7 (iv)).

In Fig. 8, we plot the half-value widths of the first peaks of KI and RbBr, as measured by Fesefeldt, Fischer and Martienssen at various temperatures. The temperature dependences are in qualitative agreement with the curve of Fig. 5, showing a tendency of bending downward from the linear curves $H \propto T$ (extrapolated

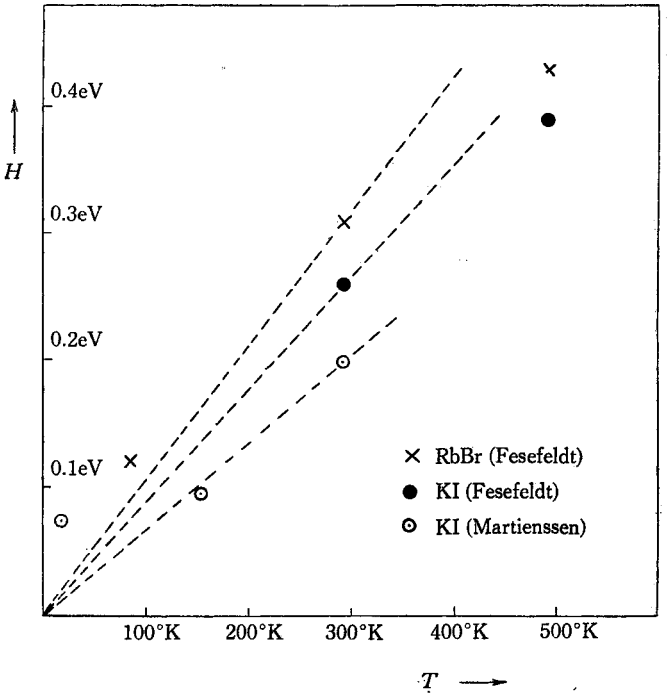

Fig. 8. The observed half-value widths H of the first peaks of Rb Br and KI at various temperatures (after Fesefeldt and Martienssen).

* Fischer carried out the experiments on KI containing varions amounts of KF. Here we confine ourselves to his specimens containing 10 mole % KF, because his data are most detailed for these, and in addition, the absorption curves seem to be almost the same as in pure KI specimens.

from room temperature values), at high temperatures where the absorption bands are, in fact, Gaussian. The reason for the discrepancy between Fesefeldt's and Martienssen's data is not clear, but it might be due to some kinds of crystal imperfections contained in the former experiment.

(ii) We now proceed to somewhat detailed analysis of Fischer's data on KI. The results of analysis of the first absorption peak are shown in Tab. 1 and Fig. 9. In the first column of Tab. 1, the specimens are arranged in the order of increasing imperfections. We can take the peak shift as a measure for the imperfection density because of (7·13), (7·20) and (7·21) (all of these quantities are proportional to T in the case of temperature variation), though the proportionality constant in the region L is different from that in the region G. In the last column the area defined by const.$\times$ (peak height) $\times$ (half-value width) are shown. In the L region, the constant is taken to be $\sqrt{\pi}\ln 2$ times of that in the G region (compare (4·7) and (5·6)).

In the Lorentzian region, H, $\mathscr{A}$, η and shift are expected to be proportional to each other according to (iv) of § 7. This relation is approximately satisfied for the specimens (f), (e) and (d), as is seen from Fig. 9. Making use of the values of H for (f) and (e), the area for the ideal crystal (which means that $H=0$, and is physically not attainable because of zero-point vibration) is extrapolated to be 0.150. For the specimen (e), therefore, we have $\eta=(0.198-0.150)/0.150=0.32$, while $\mathscr{A}=-0.08$. Substituting these in (7·14) and (7·15) we have $p=-0.45$, and further comparing (7·12) with the experimental value for (e), we get $b=0.40$ eV. The peak shift between (f) and (e) is estimated, by (7·13), to be $\Delta=+0.012$ eV whereas the observed value is $\Delta=-0.004$ eV. This discrepancy would be mainly due to the *interband* effect (7·20), which is certainly negative for the first exciton band.

In the Gaussian region, the peak separation is rather poor, and we have analysed the absorption curve only on the low energy side; the values of H for (b) and (a) were obtained by assuming the sym-

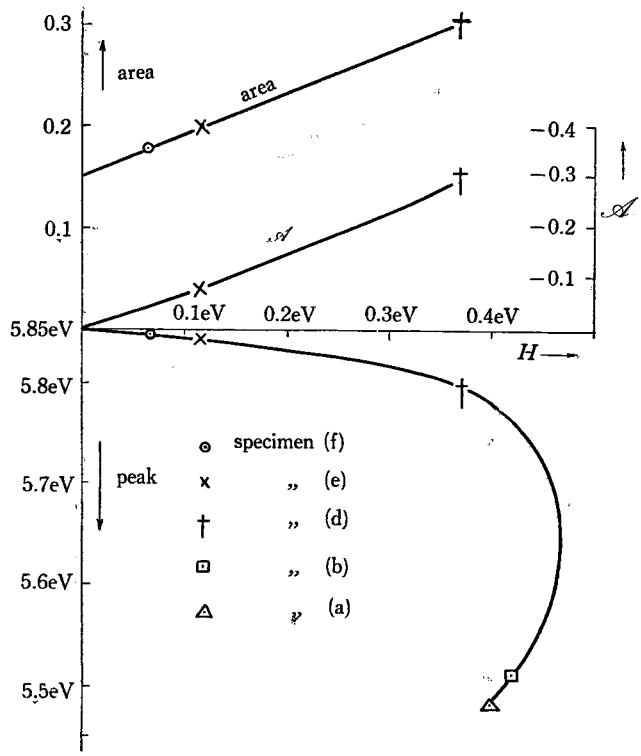

Fig. 9. The area, the asymmetry $\mathscr{A}$ and the peak position as functions of the half-value width H (see Table 1).

metry of the curve, though this is rather doubtful. The saturating or decreasing tendency of H, as the imperfection increases, is, however, well established from this data, and this is in accordance with the theoretical result (7·22). The second exciton peak of KI is separated from the first peak by $\delta\sim 0.5$ eV. We can write the shift of the first peak as $\Delta'=-\nu D^2/\delta$ in view of (7·21) and (5·4), where $\nu(>0)$ is a dimensionless quantity of the order unity. Consequently we get $H\sim 2(D^2-\Delta'^2)^{1/2}=2\{-(\delta/\nu)\Delta'-\Delta'^2\}^{1/2}$, and the maximum of H is to be realized at $\Delta'(\mathrm{m})=-\delta/2\nu$ with $H(\mathrm{m})=\delta/\nu$. From Fig. 9 we estimate $H(\mathrm{m})\sim 0.47$ eV and $\Delta'(\mathrm{m})\sim -0.20$ eV, though with some ambiguity. The relation $H(\mathrm{m})=-2\Delta'(\mathrm{m})$ is approximately satisfied. On the other hand we have $D(\mathrm{m})=H(\mathrm{m})/\sqrt{2}\sim 0.33$ eV, and according to (7·11), $s(\mathrm{m})\sim 5$, the result which is consistent with our assumption that this neighbourhood is well in the region G.

(iii) Let us now compare the observed and calculated half-value widths. According to Martienssen's data, the first peak of KI shifts to low energy side by 0.10 eV and the half-value width increases by 0.10 eV as the temperature is raised from 155°K to 293°K. According to Fischer's experiment (Tab. 1), the ratio of the peak shift to the increment of H is 1/12 for (f) − (e) and 1/6 for (f) − (d). Thus the most part ($\sim$0.09 eV) of the temperature shift of the peak is considered to be due to thermal expansion, the remaining part ($\sim$0.01 eV) being due to the dynamical lattice vibrations (self-energy). Making use of thermal expansion coefficient (linear) $0.4\cdot 10^{-4}$ deg^{-1}, we estimate the deformation potential: $E_1=-0.09$ eV$/(3\times 0.4\times 10^{-4}\times 138)=-5.4$ eV, $C=-(3/2)\times E_1=8.1$ eV. If we take the effective mass approximation, this C corresponds to C_e-C_v, because the exciton energy band shifts by $E_{1c}\Delta-E_{1v}\Delta$ when the conduction band shifts by $E_{1c}\Delta$ as a whole and the valence band by $E_{1v}\Delta$ (Here Δ means the dilation).

In this connection it is to be noted that Kawamura[38] has calculated the deformation potential for the conduction band of KCl crystal by the cellular method with result $E_{1c}=-5.4$ eV. It would presumably be smaller for KI crystal. On the other hand, E_{1v} would be of the order of $+Me^2/3a=2.4$ eV for KI (M: Madelung constant, a: lattice constant) because each of valence band electrons is considered to be fairly localized on a halogen ion. Thus the value $E_1=-5.4$ eV can be reasonably explained.

Comparing (7·12), (7·11) and (7·8) with Martienssen's data $H=0.20$ eV at $T=293$°K, and inserting $C=8.1$ eV, $Mu^2/v_0=c_{ii}=0.25\cdot 10^{12}$ dyne cm^2 (we follow the procedure due to Bardeen and Shockley[15] in evaluating c_{ii}; as for the elastic constants see ref. (29)), $b=0.40$ eV and $p=-0.45$, we get $w^{(e)}/w_0=0.62$. This means that the radius of the exciton is slightly larger than the lattice constant, which seems plausible in the case of alkali-halides.

According to (7·8), the low temperature value of H should be (θ_0/T) times the value at a high temperature T (still in the L region). Comparing Fischer's data $H=0.067$ eV (the specimen (f) at 20°K) with Martienssen's data at $T=293$°K stated above, we get $\theta_0=99$°K. On the other hand, the Debye temperature $\theta_D=\hbar u w_0/\kappa$ is estimated to be 190°K. Now, θ_0 must be smaller than $\theta_D/2$ according to the general theory. If we use (7·9) θ_0 is estimated to be 40°K. Although this estimation has

only qualitative meaning, the observed H at 20°K seems too large to be explained by the zero-point lattice vibration alone. This discrepancy is presumably due to a small amount of imperfections frozen in, in an inevitable way, on cooling the crystal, the fractional contribution of which is larger for lower temperatures. We must also add that, of Fischer's data, we are analysing only those specimens which contains 10 mol % of KF.

(iv) In the above, we have neglected the *inter*band effect (except in the Gaussian case). This effect is presumably not small, as is pointed out in (ii) in connection with the peak shift, and consequently the estimated values of b and p are of only qualitative meaning. Moreover, the true width of the energy band might be larger than b, because the latter is the width of that part of the energy band which is connected with the point $\boldsymbol{K}=0$ through the transition coefficient $\beta(\boldsymbol{K})$ of appreciable magnitude. b may be much smaller than the true width of the energy band if the exciton radius is large, while they do not differ very much for the case of alkali-halides.

On the other hand, the band bottom $\varepsilon_{\lambda b}$ is estimated, according to (ii), to lie $(1-p)b/2=0.29$ eV below $\varepsilon_{\lambda 0}$. This is consistent with the observed value 0.32 eV for the energy difference between the first peak and the β-absorption peak.[30] The latter corresponds to the creation of an exciton which is trapped in the neighbourhood of the F-center, and the required energy must be smaller than $\varepsilon_{\lambda b}$ by a trapping energy.

Here we should like to refer also to Howland's[31] calculation on the energy band structure of KCl, according to which the valence band is fairly narrow ($\sim$1 eV) and the uppermost branch has a maximum on a (011) direction nearly midway between the center and the edge of the first Brillouin zone. Making use of his result, and assuming that the bottom of the conduction band is at $\boldsymbol{K}=0$ with effective mass equal to the true electron mass, the procedure described in (2·2)$\sim$(2·9) leads to an exciton energy band which is fairly narrow and whose bottom is coincident with the top of the valence band in $\boldsymbol{K}$-space. The situation would be qualitatively the same for KI (apart from the large spin-orbit splitting of the valence band[32]). This rather speculative consideration is consistent with the result of the above analysis.

(v) According to Martienssen,[25] the first exciton peak of CsI is followed by the second and third peaks with rather small gaps, and shows, at the same time, a strong asymmetry ($\mathscr{A}=-0.23$ even at 20°K; compare with the specimen (f) of KI in Tab. (1). It is very probable that this strong asymmetry is largely due to the interband effect. In the data of Philipp and Taft,[33] the temperature dependence of the separation between the first peak and the other two peaks is well expressed by the formula $\alpha+\gamma T$ where $\alpha=0.21$ eV and $\gamma=6.4\cdot10^{-4}$ eV/K°. These values of $\mathscr{A}$ and γ are reasonably explained by (6·6) and (7·20) if we assume that the *inter*band exciton-lattice coupling constant is as large as the *intra*band one.

(vi) In Cu_2O crystal, three hydrogenlike series of absorption lines are observed,[34) 35] which are interpreted by Gross and Nikitine to be due to excitons. Each line has a very small width H, of the order of 10^{-3} eV at most.[35] This might be partly due to the large radius[35] of the exciton which makes $(w^{(e)}/w_0)^3$ of (7·8) fairly small, and partly

due to the smallness of C itself (note that $H \propto C^2$). In fact, the temperature shifts of the series limits[35] are as small as one tenth of that of the first peak in KI, thus leading to a small deformation potential.

(vii) In the case of an X-ray exciton, the hole corresponds to the innermost shell of an atom, and the effective mass m_h is very large. In this case, the dipole-dipole interaction of the Heller-Marcus[36] type might be more important in determining the effective mass m^* of the exciton; nevertheless m^* would be large unless the oscillator strength for the transition is as large as ~ 1. Thus we expect that the absorption peak corresponding to an X-ray exciton is of a Gaussian type for any temperature.

The experimental data for KCl due to Kiyono,[37] as well as that due to Trischka[38] seem to support this conclusion, as has also been noted by Parratt and Jossem,[39] although a quantitative analysis of the line shape is rather difficult in the present stage of X-ray spectroscopy. The observed half-value widths ($2 \sim 3$ eV), on the other hand, seem to be too large to be explained by the exciton lattice interaction alone.

In conclusion, the author would like to express his sincere thanks to Profs. T. Matsubara, K. Tomita and R. Kubo for stimulating discussions, and to Prof. S. Kiyono for various information on the experimental works. He is also greatly indebted to Dr. F. Fischer, the University of Göttingen, for kindly sending him detailed experimental data which have been quite stimulus and useful.

References

1) J. Frenkel, Phys. Rev. **37** (1931), 17; 1276.
2) A. von Hippel, Zeits. f. Phys. **101** (1936), 680.
3) J. C. Slater & W. Shockley, Phys. Rev. **50** (1936), 705.
4) G. Wannier, Phys. Rev. **52** (1937), 191.
5) T. Muto and H. Okuno, Journ. Phys. Soc. Japan **11** (1956), 633; **12** (1957), 108.
T. Muto and S. Oyama, Journ. Phys. Soc. Japan **12** (1957), 101.
6) D. L. Dexter, Phys. Rev. **83** (1951), 435; **108** (1957), 707.
7) A. W. Overhauser, Phys. Rev. **101** (1956), 1702.
8) Y. Takeuchi, Prog. Theor. Phys. **18** (1957), 421.
9) H. J. G. Meyer, Physica **22** (1956), 109.
10) H. Haken, Nuovo Cim. **10** (1956), 1230; Zeits. f. Phys. **146** (1956), 527; **147** (1957), 323.
See also, the review articles by H. Haken, in "*Halbleiterprobleme* IV", where a comprehensive survey and literatures are given on the exciton problem.
11) A. I. Ansel'm and Iu. A. Firsov, Journ. Exp. Theor. Phys. **28** (1955), 151; **30** (1956), 719.
12) R. E. Peierls, Ann. Phys. **13** (1932), 905.
13) Y. Toyozawa, Prog. Theor. Phys. **19** (1958), 214.
14) A. Sommerfeld and H. Bethe, *Handbuch der Physik* (1933), **24**/2.
15) J. Bardeen and W. Shockley, Phys. Rev. **80** (1950), 102.
16) H. Fröhlich, Advances in Physics **3** (1954), 325.
17) R. Kubo, Phys. Rev. **86** (1952), 929.
M. Lax, Journ. Chem. Phys. **20** (1952), 1753.
18) R. Kubo and Y. Toyozawa, Prog. Theor. Phys. **13** (1955), 160.
19) W. Heitler, *The Quantum Theory of Radiation* (Oxford, 1954), § 16.
20) L. van Hove, Physica **21** (1955), 517.
21) R. E. Peierls, Zeits. f. Phys. 88 (1934), 786. See also, *Quantum Theory of Solids* (1955), Chapt. VI.

22) F. Seitz, Phys. Rev. **73** (1948), 549.
23) R. Kubo and K. Tomita, Journ. Phys. Soc. Japan **9** (1954), 888.
24) H. Fesefeldt, Zeits. f. Phys. **64** (1930), 623.
25) W. Martienssen, Journ. Phys. Chem. Solids **2** (1957), 256.
26) S. Tutihasi, Phys. Rev. **105** (1957), 882.
27) F. Fischer, Zeits. f. Phys. **139** (1954), 328.
28) H. Kawamura, Journ. Phys. Chem. Solids, to be published.
29) Hearmon, Rev. Mod. Phys. **18** (1946), 409.
30) C. J. Delbecq, P. Pringsheim and P. Yuster, Journ. Chem. Phys. **19** (1951), 574; **20** (1952), 746.
W. Martienssen, Zeits. f. Phys. **131** (1952), 488.
31) L. P. Howland, Quarterly Prog. Rep. M.I.T. No. 23 (1957), 23.
32) N. F. Mott and R. W. Gurney, *Electronic Processes in Ionic Crystals* (Oxford, 1940), Chapt. III.
33) H. R. Philipp and F. A. Taft, Journ. Phys. Chem. Solids **1** (1956), 159.
34) M. Hayashi and K. Katsuki, Journ. Phys. Soc. Japan **7** (1952), 599.
S. Nikitine, Helv. Phys. Acta **28** (1955), 307.
J. H. Apfel and L. N. Hadley, Phys. Rev. **100** (1955), 1689.
35) E. F. Gross, Nuovo Cim. **3** (1956), Suppl. 672.
36) W. R. Heller and A. Marcus, Phys. Rev. **84** (1951), 809.
37) S. Kiyono, Sci. Rep. Tôhoku Univ. **36** (1952), 1.
38) J. W. Trischka, Phys. Rev. **67** (1945), 318.
39) L. G. Parratt and E. L. Jossem, Phys. Rev. **97** (1955), 916.